

22005



National Library of Canada

Bibliothèque nationale du Canada

CANADIAN THESES ON MICROFICHE

THÈSES CANADIENNES SUR MICROFICHE

NAME OF AUTHOR/NOM DE L'AUTEUR Stanley Michael Wiatr

TITLE OF THESIS/TITRE DE LA THÈSE Pre-Fertilization ovule ontogeny and nutrition in the garden pea.

UNIVERSITY/UNIVERSITÉ Univ. of Alberta, Edmonton

DEGREE FOR WHICH THESIS WAS PRESENTED /
GRADE POUR LEQUEL CETTE THÈSE FUT PRÉSENTÉE M.Sc.

YEAR THIS DEGREE CONFERRED/ANNÉE D'OBTENTION DE CE DEGRÉ 1974

NAME OF SUPERVISOR/NOM DU DIRECTEUR DE THÈSE DR. DAVID D. CASS

Permission is hereby granted to the NATIONAL LIBRARY OF CANADA to microfilm this thesis and to lend or sell copies of the film.

L'autorisation est, par la présente, accordée à la BIBLIOTHÈQUE NATIONALE DU CANADA de microfilmer cette thèse et de prêter ou de vendre des exemplaires du film.

The author reserves other publication rights, and neither the thesis nor extensive extracts from it may be printed or otherwise reproduced without the author's written permission.

L'auteur se réserve les autres droits de publication; ni la thèse ni de longs extraits de celle-ci ne doivent être imprimés ou autrement reproduits sans l'autorisation écrite de l'auteur.

DATED/DATE August 6, 1974 SIGNED/SIGNÉ Stanley M. Wiatr

PERMANENT ADDRESS/RÉSIDENCE FIXÉ c/o Dept. of Botany
Univ. of Alberta
Edmonton, Alta.

THE UNIVERSITY OF ALBERTA

PRE-FERTILIZATION OVULE ONTOGENY
AND NUTRITION IN THE GARDEN PEA

by



STANLEY MICHAEL WIATR

A THESIS

SUBMITTED TO THE FACULTY OF GRADUATE STUDIES AND RESEARCH
IN PARTIAL FULFILMENT OF THE REQUIREMENTS FOR THE DEGREE
OF MASTER OF SCIENCE

IN

PLANT ANATOMY

DEPARTMENT OF BOTANY

EDMONTON, ALBERTA

FALL, 1974

THE UNIVERSITY OF ALBERTA
FACULTY OF GRADUATE STUDIES AND RESEARCH

The undersigned certify that they have read, and recommend to the Faculty of Graduate Studies and Research, for acceptance, a thesis entitled "Pre-Fertilization Ovule Ontogeny and Nutrition in the Garden Pea" submitted by: Stanley Michael Wiatr in partial fulfilment of the requirements for the degree of Master of Science in Plant Anatomy.

.....*David D. Cess*.....
Supervisor

.....*James M. Meyer*.....

.....*Royal B. Ruth*.....

Date July 31, 1974.

ABSTRACT

A study of pre-fertilization ovule ontogeny in Pisum sativum was made using improved microtechnical methods. Reexamination of megasporogenesis and megagametogenesis confirms earlier observations; the megasporocyte divides meiotically to produce a chalazal functional megaspore and three degenerative megaspores. Non-functional megaspore degradation is staggered; two chalazal megaspores are the first to degenerate while the third degenerative megaspore persists during initial expansion of the functional megaspore. An eight-nucleate, seven-celled embryo sac is produced by the functional megaspore after three sets of mitotic divisions. Ephemeral antipodals in the chalazal end of the embryo sac degenerate well before fertilization. The presence of wall ingrowths in the synergids is documented for Pisum. Nucellar degradation is closely correlated with megagametophyte expansion and follows a sequential pattern of cytological changes involving cell wall thickening, starch mobilization, wall degradation, alteration of cytoplasm, and obliteration of nucellar cell structural integrity. The possibility of gametophytic regulation of nucellar cell breakdown is discussed. Pisum ovules are bitegmic. Both integuments are initiated in epidermal cells, but subsequent differentiation is radically different. A single vascular strand enters the ovule and terminates in the outer integument. Procambium is already organized when a megasporocyte is present. Vascular differentiation is correlated with the onset of megagametogenesis, but

maturation of xylem and phloem by the time an embryo sac has organized is minimal. The relationships of integument and vascular ontogeny to embryo sac nutrition are discussed. A scheme of megagametophyte nutrition is proposed whereby the megagametophyte obtains all necessary nutrients from degenerate nucellus, in contrast to classical schemes of direct involvement by the parent sporophyte in embryo sac nutrition.

ACKNOWLEDGMENT

The thorough review and constructive criticisms of the manuscript by my adviser, Dr. David Cass, are gratefully acknowledged. His understanding and patience during its preparation alleviated much of the pressure and anxiety generated by deadlines. I am deeply indebted to my wife, Phyllis, for admirably handling the onerous task of typing the manuscript. The able technical assistance of Sherman and Valerie Nelson in constructing photographic plates is also appreciated. Research for this thesis has been supported in part by National Research Council Grant A6103 to David D. Cass.

TABLE OF CONTENTS

CHAPTER		PAGE
ONE	Introduction and Literature Review	1
TWO	Pre-Fertilization Ovule Ontogeny	10
	Introduction	10
	Material and Methods	12
	—Cultivation of plants	12
	Microtechnique	13
	Results	17
	Megasporogenesis and megagametogenesis	17
	Megaspore mother cell	17
	Four megaspores	18
	Non-functional megaspore degeneration	19
	Two nucleate gametophyte	19
	Four and eight nucleate gametophytes	20
	Organization of the mature embryo sac	21
	Central cell	21
	Antipodals	22
	Synergids	22
	Egg cell	24
	Nucellus	24
	Integuments	29
	Inner integument	29
	Outer integument	31
	Vasculature	32
	Discussion	35

	PAGE
Bibliography	78
Appendix	83

LIST OF FIGURES

Figure	Page
1. Light micrograph of ovule primordium with sporogenous cells.	50
2. Light micrograph of young ovule with a differentiated megasporocyte.	50
3. Light micrograph of nucellus with a megasporocyte at early prophase.	50
4. Light micrograph of ovule vasculature at the megasporocyte stage.	50
5. Electron micrograph of nucellar epidermal and hypodermal cells.	52
6. Electron micrograph of surface detail of the nucellar epidermis.	52
7. Electron micrograph of plasmodesmata in contiguous walls of nucellar epidermal cells.	52
8. Light micrograph of enlarging chalazal megaspore.	52
9. Light micrograph of cytoplasm of enlarging megaspore.	52
10. Electron micrograph of inner integument primordium	52
11. Electron micrograph of inner integument-nucellus junction.	52
12. Light micrograph of ovule with four megaspores.	54
13. Light micrograph of chalazal nucellus of an ovule at four megaspore stage.	54
14. Light micrograph of micropylar region of nucellus at four megaspore stage.	54.
15. Light micrograph of procambial strand in the ovule at four megaspore stage.	54

Figure	Page
16. Light micrograph of funicular procambium at four megaspore stage.	56
17. Light micrograph of two nucleate gametophyte.	56
18. Light micrograph of young two nucleate gametophyte prior to migration of nuclei.	56
19. Light micrograph of two nucleate gametophyte after vacuole formation.	56
20. Light micrograph of two nucleate gametophyte and nucellar tissue.	56
21. Light micrograph of entire ovule with two nucleate gametophyte.	58
22. Light micrograph of chalazal nucellus in ovule at two nucleate gametophyte stage.	58
23. Light micrograph of transverse section through a two nucleate gametophyte.	58
24. Light micrograph of ovule vasculature at the two nucleate gametophyte stage.	58
25. Light micrograph of funicular procambium at two nucleate gametophyte stage.	60
26. Light micrograph of micropylar cytoplasm in a four nucleate gametophyte.	60
27. Light micrograph of four nucleate gametophyte and inner integument (paraffin).	60
28. Light micrograph of transverse section through micropyle.	60
29. Light micrograph of early four nucleate gametophyte, nucellus, and inner integument.	60
30. Light micrograph of late four nucleate gametophyte, nucellus, and inner integument.	60

Figure	Page
31. Light micrograph of micropylar slit formed by the outer integument.	62
32. Light micrograph of funicular vasculature in ovule at four nucleate gametophyte stage.	62
33. Light micrograph of chalazal nucellus at late four nucleate gametophyte stage.	62
34. Light micrograph of ovule vasculature at four nucleate gametophyte stage.	62
35. Light micrograph of ovule with an eight nucleate gametophyte.	62
36. Light micrograph of chalazal cytoplasm of an eight nucleate gametophyte.	64
37. Light micrograph of micropylar cytoplasm of an eight nucleate gametophyte.	64
38. Light micrograph of ovule vasculature at eight nucleate gametophyte stage.	64
39. Light micrograph of chalazal nucellus in an ovule with a differentiating embryo sac.	64
40. Light micrograph of funicular vasculature at eight nucleate gametophyte stage.	64
41. Light micrograph of embryo sac (paraffin).	66
42. Light micrograph of ovule with embryo sac near maturity.	66
43. Light micrograph of differentiating megagametophyte after polar nuclei have migrated.	66
44. Light micrograph of a mature embryo sac.	66
45. Electron micrograph of polar nucleus after migration.	69
46. Electron micrograph of rough endoplasmic reticulum in central cell cytoplasm.	69

Figure	Page
47. Electron micrograph of lateral embryo sac wall.	69
48. Light micrograph of antipodal cells during megagametophyte differentiation.	69
49. Light micrograph of chalazal end of embryo sac after antipodal degradation.	69
50. Light micrograph of egg apparatus near maturity.	69
51. Light micrograph of micropylar area of the megagametophyte during megagametophyte differentiation.	69
52. Light micrograph of synergid cells during megagametophyte differentiation.	69
53. Light micrograph of egg apparatus in a differentiating megagametophyte.	69
54. Light micrograph of wall ingrowths in synergid cells of a mature egg apparatus.	69
55. Light micrograph of wall ingrowths in the micropylar wall of a synergid cell.	69
56. Electron micrograph of inner integument in ovule at embryo sac stage.	71
57. Light micrograph of nucellar tissue proximal to the chalazal end wall of an immature embryo sac.	71
58. Light micrograph of chalazal nucellus when a mature embryo sac is present.	71
59. Light micrograph of transparent areas at micropylar ends of synergids.	71
60. Electron micrograph of synergid-synergid and synergid-central cell wall material.	71
61. Electron micrograph of degenerating nucellar cell walls.	73

Figure	Page
62. Electron micrograph of rough endoplasmic reticulum in a degenerating nucellar cell.	73
63. Electron micrograph of vacuolate cytoplasm in a degenerate nucellar cell.	73
64. Electron micrograph of inner-outer integument interface.	73
65. Light micrograph of ovule vasculature in an ovule containing a mature embryo sac.	73
66. Light micrograph of funicular vasculature when a mature embryo sac is present.	73
67. Electron micrograph of electron dense material separating the inner integument from degenerate nucellar cells.	73
68. Light micrograph of ovule vasculature when a mature embryo sac is present (transverse section).	73
69. Fluorescence micrograph of ovule with a megaspore mother cell.	75
70. Fluorescence micrograph of ovule with an enlarging functional megaspore.	75
71. Fluorescence micrograph of ovule with a four nucleate gametophyte.	75
72. Fluorescence micrograph of ovule with an eight nucleate gametophyte.	75
73. Fluorescence micrograph of ovule with a mature embryo sac.	75
74. Histogram of changes in nucellus, megasporocyte, functional megaspore, and megagametophyte lengths during megasporogenesis and megagametogenesis.	77
75. Schematic representation of possible routes of nutrient entry into the embryo sac.	78

CHAPTER ONE — INTRODUCTION

Gametophytes of lower vascular plants are free-living organisms physically detached from the parent sporophyte. Spores shed from the sporophyte germinate in a suitable environment producing plants which in some species photosynthesize (e.g. fern gametophytes) or species which may be subterranean and associated with an endophytic fungus (e.g. Lycopodium gametophytes) (Foster and Gifford 1959). Since the two generations are not physically attached, it is patently reasonable to assume the parent sporophyte is not involved in gametophyte nutrition. However, the complexity and intimate association of sporophytic structures associated with reproduction in angiosperms would make a similar assertion for flowering plant megagametophytes untenable. Angiosperm megagametophytes are enclosed throughout ontogeny by amounts and forms of sporophytic tissue which differ from species to species. The ovule forms the immediate environment of the megagametophyte, and although highly variable among angiosperms, it is generally considered to consist of a sporangium surrounded by one or more integuments (Esau 1965). Since the megagametophyte is retained and enclosed in sporophytic tissue it is reasonable to expect a mode of nutrient supply unlike lower vascular plant gametophytes. It has been suggested that the megagametophyte of seed plants is developmentally distinct from the sporophyte (as in lower vascular plant gametophytes), but has also evolved to be physiologically dependent on the sporophyte

(Diboll and Larsen 1966). In assuming direct sporophytic involvement in megagametophyte nutrition, Newcomb (1972) recognized three aspects of embryo sac nutrition:

1. pathways of metabolites into the sporophytic tissue surrounding the embryo sac
2. subsequent passage of metabolites into the gametophytic tissue
3. nutritional relationships of cells within the embryo sac.

Pathways into sporophytic tissue—The most conspicuous pathway of nutrient entry into sporophytic tissue of the ovule is via a vascular strand generally found in the funiculus (Maheshwari 1950). The extent of vascular development is, however, highly variable. Vascular tissue may terminate at the chalaza or extend into one or more integuments (Maheshwari 1950). Where a vascular strand enters an integument, it may extend the entire length (e.g. Zizyphus, Kajale 1944) or it may terminate well before the morphological apex of the ovule as in Pisum. Complex arrays of branching and anastomosing bundles have been reported in Hymenocallis occidentalis (Whitehead and Brown 1940) although less intricate vascular systems, usually a single trace, are more commonly found. Vascular tissue in ovules is primary and suggested to be in a functioning state during seed maturation (Esau 1965).

Passage to gametophytic tissue—The subsequent passage of nutrients from the terminus of the vascular strand in the ovule to the female gametophyte presumably occurs via

an axial, chalazal route through nucellar cells, or laterally through an integumentary tapetum (endothelium) which could mediate the flow of metabolites (see fig. 75) (Subramanjam 1960; Johri 1962; Masand & Kapil 1966; Linskens 1969).

A chalazal route of nutrient entry has been suggested with the observation of axially elongate and densely cytoplasmic nucellar cells which may facilitate nutrient transport to the embryo sac (Subramanjam 1960). The walls of these cells are slightly thickened as in certain members of the Lythraceae (Joshi and Venkateswarlu 1935, 1936) or thin-walled as in Lobelia cardinalis (Cooper 1942).

Nucellar tracheids have been observed in the chalazal nucellus of Castanea (Benson 1894), Asclepias (Frye 1902), and Carpinus (Benson et al 1906). However, these cells were not continuous with the vascular supply of the ovule. In Anacolosia frutescens and Strombosia zeylanica Fagerlind (1947) observed that the vascular supply of the ovule extended through the chalazal nucellus to the base of the embryo sac. While both nucellar tracheids and nucellar vascular strands provide morphological evidence for a chalazal route of nutrient flow to the embryo sac in these two species, it is apparent that they also represent highly specialized structures uncommon to the majority of angiosperms which have been investigated.

A lateral flow of nutrients to the embryo sac has been suggested due to the presence of an endothelium which is usually continuous with the embryo sac (Maheshwari 1950). Newcomb (1972) suggested that the endothelium of sunflower

may be involved in embryo sac nutrition because of its position adjacent to the embryo sac and the occurrence of many organelles associated with synthesis in endothelial cells. Subramanjam (1960) also regards the endothelium as a mediator of nutrient flux to the embryo sac although the peculiar if not contradictory example of Lobelia trigona was noted where tapetal cells become thick-walled and apparently impervious when a mature embryo sac is present (Kausik 1935). Nevertheless, many investigators suggest there is little doubt that the endothelium plays an important role in embryo sac nutrition (see Maheshwari 1950; Subramanjam 1960).

Nutritional relationships of embryo sac cells—The egg of Plumbago capensis has been implicated in embryo sac nutrition. (Cass 1972). The appearance of a filiform apparatus and the timing of its formation suggested the possibility of a nutritional role for the egg cell. However, it was noted that the egg cell may be a special case of reduction where gametic and synergid functions are combined since the egg apparatus of P. capensis lacks synergids.

The central cell has been considered a suitable gametophytic component in obtaining nutrients from the immediate environment of the embryo sac since the wall of the gametophyte is in contact with nucellus cells which usually degenerate during megagametogenesis (Subramanjam 1960). The recent discovery of embryo sac wall ingrowths in Helianthus (Newcomb and Steeves 1970), Capsella (Schulz and Jensen 1968b), Pisum (Marinos 1970), and Lobelia

(Torosian 1971) and the possible role of such ingrowths in facilitating short distance transport of solutes (Gunning and Pate 1969) supports the notion of an absorptive function for the central cell. It is also significant that plasmodesmata have not been observed in the embryo sac wall of Zea (Diboll and Larsen 1966), Helianthus (Newcomb and Steeves 1971), and Petunia (Went 1970) since their absence indicates a developmental distinctness of the megagametophyte.

The timing of formation of central cell wall ingrowths warrants a cautious interpretation of their possible role in embryo sac nutrition. Newcomb and Steeves (1971) noted the appearance of embryo sac wall ingrowths in sunflower during synergid wall formation, whereas new wall material was deposited over the projections during embryogenesis. This is in contrast to the formation of wall ingrowths in Capsella which are initiated after fertilization and continue to proliferate during early embryogeny (Schulz and Jensen 1968b, 1969). Similarly, massive embryo sac wall ingrowths in Pisum appear to be associated with embryonic rather than embryo sac nutrition (Marinos 1970). It is apparent that a distinction should be made regarding the functional significance of central cell wall ingrowths as they may relate to either female gametophyte nutrition and/or embryo nutrition depending on the time of development at which they occur.

Synergid cells have been ascribed a secretory or absorptive function by many investigators (Van der Pluijm

1964: Jensen 1965: Diboll 1968: Schulz and Jensen 1968a: Newcomb 1972). As with other embryo sac components their exact function is unresolved, and while it appears that many authors assume synergids direct pollen tube growth by secreting a chemotropic factor, only the work regarding synergids as cells involved in megagametophyte nutrition will be treated here.

Wall ingrowths in the synergids of numerous species have been a key morphological character in suggesting an absorptive (or secretory) role for these cells because of a greatly increased surface to volume ratio (see Gunning and Pate 1969). Large numbers of mitochondria and dictyosomes and large amounts of endoplasmic reticulum were observed in the synergid cytoplasm of Gossypium (Jensen 1965) and Capsella (Schulz and Jensen 1968a). The abundance of these cytoplasmic components suggested metabolically active cells which were interpreted by these authors to be a strong indication of cells specialized in the absorption and transport of compounds from the surrounding integuments. The synergids of Helianthus annuus are situated in a micropylar outpocketing placing them in close proximity to the vasculature of the placenta (Newcomb 1972). Newcomb considered this positioning suitable for an absorptive or secretory role. Subramanjam (1960) noted the occurrence (in Allium spp. and some cucurbits) of persistent synergids which presumably behaved as haustoria.

With few exceptions (see Maheshwari 1950) the physiological role of synergids is limited from the time of

their differentiation to the time of their disorganization; in Gossypium (Jensen and Fisher 1968) and Hordeum vulgare (Cass and Jensen 1970) one synergid degenerates shortly before fertilization, while the degeneration of both synergid cells occurs after fertilization in Petunia (Went 1970a) and Capsella (Schulz and Jensen 1968a).

The number, structure, and persistence of antipodals is highly variable among angiosperms (Maheshwari 1950). Although no agreement exists on antipodal function many authors have assigned a nutritional role to these cells (see Subramanjam 1960; Masand and Kapil 1966). That antipodals function as gametophytic nutritional devices appears to be a favored interpretation because of their characteristic location at the chalazal end of the embryo sac; this position is amenable to nutrient uptake via a chalazal route of entry through sporophytic tissue. Ultrastructural investigations of antipodals have led to a similar conclusion (Diboll and Larsen 1966; Newcomb 1972). Diboll and Larsen suggested that the antipodals of maize might be involved in the movement of large amounts of nutritive material because of the presence of papillate wall projections and an abundance of cytoplasmic organelles interpreted as evidence for high respiration coupled with synthetic activity. Sunflower antipodals also contained wall projections and numerous organelles related to synthetic activity (Newcomb 1972). Moreover, the presence of plasmodesmata in the antipodal cells bordering the integument cells strengthened the interpretation that sunflower antipodals function in

nutrient uptake. However, the persistence of antipodals in maize and sunflower was notably different. In sunflower, the antipodals began to degenerate shortly before fertilization, whereas in maize the antipodals persisted and apparently underwent a post-fertilization increase in metabolic activity. It has been suggested that persistent antipodals may be important in the early stages of endosperm development, particularly in grasses (Brink and Cooper 1944), while nutritional activity may be shifted to some other embryo sac component(s) in those plants having ephemeral synergids (Diboll 1968). The interpretation of antipodals as nutritional devices in the majority of plants investigated appears to be distinct from the infrequent occurrence of antipodal haustoria which elongate considerably to form tubular, occasionally branched processes (see Maheshwari 1950; Subramanjam 1960).

The principle of gametophytic dependence on the sporophyte is well established in the literature (Diboll and Larsen 1966), yet the absence of correlative developmental studies investigating the entire ovule as an interacting system is surprising. Limitations imposed by classical techniques of preparation and interest restricted to the female gametophyte or embryo no doubt contributed to the scarcity of information. This study was undertaken to examine the developmental anatomy of the garden pea ovule prior to fertilization, with attention given to proposed routes of nutrient entry into the female gametophyte. The common garden pea (Pisum sativum L.) was selected because

of the relative ease of obtaining sufficient material for examination and the earlier work of G.O. Cooper (1938) which indicated a common type of megagametophyte development.

/

CHAPTER TWO—PRE-FERTILIZATION OVULE ONTOGENY

Introduction

Details of megasporogenesis and megagametogenesis in Pisum sativum L. were first described by Roy (1933) and G.O. Cooper (1938). Although Cooper disagreed with Roy on the derivation of the megasporocyte, they were in general agreement regarding the subsequent pattern of megasporogenesis and megagametogenesis in that it conformed to the Polygonum type of embryo sac development according to Maheshwari's (1950) classification. D.C. Cooper's (1938) observations of the mature embryo sac of Pisum agree with those of G.O. Cooper. Briefly, the female gametophyte was described as an eight-nucleate, seven-celled structure with three antipodal cells, a binucleate central cell, and an egg apparatus consisting of two synergid cells and an egg cell. D.C. Cooper (1938) also noted degeneration of antipodals soon after fertilization.

Post fertilization development and embryogenesis have been described by D.C. Cooper (1938), Reeve (1948), and Marinos (1970a,b). The work of Marinos is particularly interesting since he described a post-fertilization increase in embryo sac volume commensurate with an overall increase in ovule size. Extensive embryo sac wall ingrowths and large intercellular air spaces in the ovular tissue were also observed in the vicinity of the proembryo. Marinos suggested this organization, together with involvement

of endospermic cytoplasm, related to transport and metabolism of materials derived from ovular tissue.

Only scant, ancillary information is available about the structure of ovule components in Pisum. G.O. Cooper (1938) noted the appearance of inner and outer integument primordia when a megasporocyte was present, and subsequent differential growth of integuments such that the ovule curved toward the style at maturity. Davis (1966) described Papilionaceous ovules as generally bitegmic, crassinular, and having a zigzag micropyle.

In this study of ovule ontogeny and gametophyte nutrition, classically prepared paraffin material has been included for comparative purposes. However, new information obtained with use of improved microtechnical methods warranted reexamination of megasporogenesis and megagametogenesis. Nucellus, inner integument, outer integument, and vascular ontogeny are treated separately, but are related to specific stages of megasporogenesis or megagametogenesis. Such an assessment of the development and function of ovule components should generate a better understanding of the ovule as a developmental system, particularly as it relates to the nutrition of the female gametophyte.

Materials and Methods

Cultivation—Seeds of Pisum sativum L. var Homesteader Lincoln were obtained from the botany greenhouse at the University of Alberta. Imbibed seeds were placed between sheets of paper towels in a flat tray moistened with tap water from an inverted flask and were kept in darkness for the period of germination and early growth. After 10-12 days etiolated seedlings were produced which could be easily handled for subsequent transplanting. Root systems were routinely inoculated with "RP Inoculator" (The Rudy-Patrick Co., Inoculant Laboratories, P.O. Box 404, Princeton, Illinois) to induce nodule formation. A hydroponic culture technique was used to grow plants to harvesting age. Etiolated seedlings were transferred to one quart plastic containers with standard strength Hoagland's solution (Anon 1938) with iron supplied as FeEDTA (Steiner and Winder 1969) (Appendix 1). The pots had been painted prior to use to prevent light penetration which promoted algal growth. Plants were irrigated with Hoagland's solution at weekly intervals; after 3-4 weeks the medium was completely renewed with fresh Hoagland's solution

Plants were grown in a controlled environment chamber. The lighting system consisted of cool white fluorescent tubes and 100W incandescent bulbs. Light measurements in the center of the chamber at the top of the plants were made using a Lambda LI-185 Quantum/Radiometer/Photometer. The measurements at the end of the growth period were 310 $\mu\text{Einstein s}^{-1} \text{ M}^{-2}$, 115 Watts M^{-2} , and 20.5 Klux.

Light-dark duration was 16hr.-8hr. respectively, with an abrupt light-dark change. Air temperature was 21°C during the light period and 15°C during the dark period. Relative humidity was maintained at 50-60% at all times. Anthesis at the first flowering node occurred after ca. 5 weeks of growth in the chamber.

Microtechnique—Material prepared for paraffin sectioning was fixed in Randolph's solution (Sass 1958), dehydrated in an ethanol-tertiary butyl alcohol series (Johansen 1940), and embedded in "Paraplast-Plus" (m.p. 56°-57°C). Blocks were sectioned at 7µm on a Spencer model AO rotary microtome. Paraffin ribbons were fixed to glass slides with Haupt's adhesive (Jensen 1962). Sections were stained with safranin-fast green (Jensen 1962) or alternatively with a 0.1% aqueous solution of toluidine blue O. Both staining procedures provided good specimen contrast.

Tissue embedded in plastic was either chemically or physically fixed. Ovules or entire ovaries were fixed in 3% phosphate-buffered (pH 6.8) glutaraldehyde (Ladd Research Industries, Inc., Burlington, Vermont) for 20-24hrs. After several rinses with buffer tissue was postfixed in 2% phosphate-buffered osmium tetroxide (Ladd Research Industries Inc.) for 3hrs. Material was dehydrated in an ethanol series followed by three changes of absolute ethanol. Fixation, rinsing, and dehydration were performed at room temperature. Alternatively, material was fixed in 5% phosphate-buffered (pH 6.8) glutaraldehyde for 48hrs. at 0°C. Fixed material was dehydrated in an ethanol series

at 0°C, then transferred to propylene oxide at room temperature. Mannitol (6.3gm./100ml. fixative) was added to the fixative used for ovules from flowers weighing more than 50mg. because of a relatively high osmotic potential which is reported to develop in the embryo sac (Marinos 1970).

Tissue from both fixation procedures was infiltrated with Spurr's low viscosity resin (Spurr 1969) over a period of 3-4 days at room temperature. Slow infiltration was necessary to overcome poor infiltration which frequently occurred, particularly in the embryo sacs of older ovules. Infiltrated material was transferred to a flat embedding tray and polymerized in a vacuum oven overnight at 65°C.

Freeze substitution was employed as another method of fixation. Individual ovules, or entire carpels from very young flowers were immersed in a solution of 12% methylcyclohexane in isopentane precooled with liquid nitrogen (Jensen 1962). Dissecting ovules from carpels of very young flowers (less than 10mg.) was not necessary since very little observable ice damage was found afterwards. Frozen material was rapidly transferred into vials containing either dry methanol, or acetone precooled with dry ice. Tissue was kept at -60°C for 4-6 weeks. The substituting solvent was not changed for the duration of the substitution period because of a large solvent-material ratio. After the substitution period, material was gradually brought to room temperature and washed with a minimum of three changes of anhydrous solvent. The dehydrated

material was infiltrated with resin and polymerized as described previously for aldehyde fixation.

Sectioning, staining, microscopy—All plastic blocks were sectioned on a Reichert OM U2 ultramicrotome with a DuPont diamond knife. Sections for light microscopy were cut at 1-1.5 μm and mounted on gelatin coated glass slides (Jensen 1962). Serial sections were easily obtained with "Cenco Softseal Tackiwax" (Central Scientific Co., Chicago, Illinois) applied to the upper and lower surfaces of the specimen block.

Periodic acid-Schiff's reagent (hereafter referred to as PAS) was used to localize total insoluble polysacharides (Jensen 1962). Aniline blue-black (hereafter referred to as ABB) was employed as a non-specific protein stain (Fisher 1968).

Material for fluorescence microscopy was stained in a 0.01% acridine orange solution for 15-30 minutes. After staining, the material was briefly rinsed in running tap water and observed immediately. The recognized merit of acridine orange is in its differential affinity for nucleic acids (see Armstrong 1956; von Bertalanffy et al 1956; von Bertalanffy and Bickis 1956), but the dye also produced good morphological detail in cell walls.

Observations were made with a Zeiss photomicroscope; both bright field and phase-contrast optics were routinely used. A Super Pressure Mercury Lamp (Model HBO 200W) was the source of illumination for fluorescence microscopy. Exciter filter 1 (BG12) transmitted ultraviolet light

between 325-500nm. Barrier filters 44 and 53 allowed visible light greater than 530nm. to be transmitted, while blocking shorter wavelengths. All photographs for light microscopy were taken on Kodak Plus-X pan film processed in Microdol-X developer (1:3 dilution).

Ultrathin sections for electron microscopy were cut at 600-800Å (silver interference color) and mounted on 75 or 100 mesh formvar coated grids. A 0.3% formvar solution was best in combination with 100 mesh grids. Sections were stained in 3% uranyl acetate in 80% ethanol for one hour. After several rinses in distilled water, the grids were allowed to dry, then post-stained with Reynolds' lead citrate (Reynolds' 1963) for 10 minutes. Observations were made with a Philips EM200 at an operating voltage of 60kV.

RESULTS

Megasporogenesis and Megagametogenesis

Sporogenous cells—Ovule differentiation from placental tissue occurs early in development of the pea flower. Flowers weighing about 1mg. contain ovule primordia with sporogenous cells circumscribed by a nucellar hypodermis (fig. 1). The sporogenous cells, more or less ovoid in longitudinal view, are larger than adjacent cells. Cytoplasm is typically less dense than that of surrounding cells. Similarly, nuclei of sporogenous cells are translucent and not exceptionally well defined, whereas nuclei of vegetative cells are very ABB+. No peculiar wall characteristics or differential polysaccharide staining was observed in sporogenous cell walls.

Megaspore mother cell—The megaspore mother cell differentiates from one sporogenous cell (fig. 2,3). Its position in the nucellus was variable; lateral and micropylar surfaces were either in direct contact with the hypodermis, or separated from it by a layer of vegetative or sporogenous cells. Cytoplasm of the megasporocyte is lightly ABB+ and contains a few small starch grains. The megasporocyte nucleus is lightly ABB+, but also contains a densely ABB+ nucleolus (fig. 2,3). The nucleolus is spindle to crescent-shaped in sectional view, adjacent to the nuclear membrane, and larger than nucleoli of vegetative cells. It is considered to be diagnostic of the megasporocyte since it was observed in all megasporocyte nuclei which were examined.

As the megasporocyte enlarges its cytoplasm remains homogeneous and translucent with two vacuoles typically found in the cell (fig. 3). The vacuoles are larger than any observed earlier in its ontogeny. In one megasporocyte a small vacuole appeared to have been fusing with one of the larger vacuoles, suggesting that vacuolation occurs by a coalescence of smaller vacuoles. Although the vacuoles in fig. 3 are separated by the megasporocyte nucleus, this polarity was not constant. Other megasporocytes observed at this stage had similar vacuoles situated at either end of the cell. In early meiotic prophase, nucleoplasmic homogeneity is lost with the appearance of darkly stained areas of heterochromatin (fig. 3). The nuclear membrane also becomes very distinct at this time, forming a sharp nucleoplasm-cytoplasm boundary. The distinctive megasporocyte nucleolus persists until pachytene of meiotic prophase, but its subsequent fate could not be traced. That the peculiar nucleolus may be associated with metabolic events of meiosis is indicated by the absence of morphologically similar nucleoli in the megaspores.

Four megaspores — A tetrad of megaspores is derived from the megaspore mother cell. Both linear (fig. 12,14) and T-shaped arrangements (fig. 8) were observed. Only the orientation of the two micropylar megaspores varies; the two chalazal megaspores are always axially aligned. The chalazal megaspore is the largest and it subsequently differentiates into the female gametophyte. Cytokinesis and cross-wall formation during megasporogenesis were not

observed because of the difficulty associated with obtaining material at that stage of development. However, the large chalazal megaspore is probably derived by an unequal distribution of cytoplasm during meiosis, similar to megasporogenesis in Helianthus annuus (Newcomb 1972). The functional megaspore usually contains one large vacuole in addition to numerous granular inclusions which stain lightly with ABB. The wall of the functional megaspore does not have any unusual characteristics and appears similar in morphology and PAS intensity to subjacent cell walls.

Non-functional megaspore degeneration — Functional megaspore expansion and differentiation is accompanied by rapid degeneration of the other megaspores. This is most apparent in the two micropylar megaspores which stain intensely with ABB (fig. 8,9,70) and are often difficult to recognize as separate cells. The megaspore adjacent to the enlarging functional megaspore is somewhat more persistent and retains a well-defined nucleus in a homogeneous, translucent cytoplasm (fig. 8,70). After a two-nucleate gametophyte has differentiated, however, the persistent megaspore has degenerated like its sister megaspores (fig. 18-20).

Two-nucleate gametophyte — Prior to any significant megaspore expansion, the nucleus of the functional megaspore divides forming a two nucleate gametophyte (fig. 17,18). Shortly after the first mitotic division the gametophyte cytoplasm contains numerous vacuoles of variable

size. The two gametophytic nuclei stained differentially with ABB; one being more homogeneous and denser than the other. The ABB dissimilarity suggests a metabolic independence of the two nuclei within the coenocytic gametophyte which may be related to subsequent differentiation and organization of the embryo sac. The two nuclei migrate to the poles of the expanding cell and become separated by a large vacuole which occupies most of the cell volume (fig. 19,20). The lateral inside surfaces of the gametophyte have only a thin layer of cytoplasm connecting the two poles. A few starch grains were observed in the gametophyte cytoplasm. Large granular inclusions observed in the functional megaspore were not found at this stage. The wall of the two-nucleate gametophyte was similar to the megaspore wall with no unusual characteristics.

Four and eight nucleate gametophyte — The four and eight nucleate gametophytes are morphologically similar to the two nucleate stage. A large central vacuole separates an equal number of nuclei at either end of the central cell with numerous small vacuoles in the chalazal and micropylar cytoplasm (fig. 27,29,30). The prominent increase in size of the gametophyte from the two to eight nucleate stage is concurrent with the degradation of nucellar tissue. At the site of the egg apparatus the micropylar region of the female gametophyte extends beyond the apex of the inner integument such that the micropylar end wall lies next to the inner epidermis of the outer integument after any remaining nucellar cells have been digested (fig. 30,35,43).

Lateral walls of the enlarging gametophyte eventually come in contact with the epidermis of the inner integument, while the chalazal area remains embedded in nucellar tissue..

Organization of the mature embryo sac — The eight-nucleate coenocytic gametophyte reorganizes into an eight-nucleate, seven celled structure with three chalazal antipodal cells, two polar nuclei in a central cell, and a micropylar egg apparatus (fig. 41,42,44,50,53). Deposition of wall material in the formation of antipodal cells apparently occurs at the same time as wall formation in the cells of the egg apparatus.

Central cell — After three cells organize at each end of the embryo sac, two remaining nuclei migrate to occupy a central position along the ventral arch of the central cell (fig. 48,51,41-45). The polar nuclei remain contiguous, but do not fuse prior to fertilization. A large vacuolate nucleolus which stains darkly with ABB is found in each polar nucleus.

The thin band of cytoplasm surrounding the central cell vacuole is typically ABB+. Its most obvious ultrastructural characteristic is the presence of numerous parallel strips of rough endoplasmic reticulum (fig. 46).

The embryo sac wall lies adjacent to degenerating nucellar cells during the maturation of the megagametophyte (fig. 42-44, 72,73).. Although the wall appears uniform in the light microscope, the inside surface is very irregular, forming embayments of central cell cytoplasm (fig. 47).

The presence of wall ingrowths per se is apparently restricted to post fertilization expansion of the embryo sac (see Marinos 1970). No plasmodesmata were observed in the lateral walls of the central cell.

Antipodals — Walls surrounding the antipodals are very thin and often difficult to discern clearly (fig. 48). The cells contain dense protoplasm with poorly defined nuclei and appear flattened against the chalazal end wall of the embryo sac. Wall material around the antipodals was observed only during the early differentiation of the eight-nucleate gametophyte. Antipodal cells could not be identified in mature embryo sacs, but what appeared to be fragments of wall material were occasionally observed (fig. 49).

Synergids — The three cells located at the micropylar end of the embryo sac undergo a sequence of development in which they differentiate into a pair of synergid cells and an egg cell (fig. 50,51,53). Both synergid cells are positioned adjacent to the micropylar end wall of the embryo sac. Immediately after wall formation around the synergids, both cells contain dense cytoplasm with no apparent vacuoles (fig. 43,52). During cell enlargement and at maturity, a few vacuoles develop in the synergid cytoplasm (fig. 50,54). Generally larger vacuoles occupy a chalazal position in the cell with most of the cytoplasm and nucleus at the micropylar end of the synergid. However, this polarity was not consistent and examples were observed where a synergid nucleus and cytoplasm were situated chalazally (fig. 50).

The common wall between the two synergids extends from the micropylar base of the embryo sac chalazally and borders the egg cell wall. Numerous plasmodesmata are found in the common synergid wall as well as the chalazal wall of the synergids (fig. 60). A thin band of electron dense material is also present in the mid-region of the synergid cell walls. The micropylar region of the common wall develops wall ingrowths which project laterally into the cytoplasm of both synergids (fig. 53-55). Wall ingrowths found in synergids have been referred to as a "filiform apparatus" (van der Pluijm 1964; Schulz and Jensen 1968a), but the wall ingrowths of Pisum do not appear filiform. The wall projections are rather a reticulate mass of polysaccharide material which collectively has a lenticular morphology. Two areas of differing PAS intensity are found in the wall ingrowths (fig. 54). The wall material adjacent to the synergid cell cytoplasm reacted strongly with PAS, while the mid-region was nearly transparent. This differential reactivity to PAS suggests that structural and certainly chemical differences exist within the wall ingrowths. Occasionally, the micropylar end wall of a synergid also had a thick deposit of PAS+ material (fig. 55). Unlike the lenticular ingrowth of the common synergid wall, the end wall thickening formed a flat plate of polysaccharide material contiguous with the embryo sac end wall. At intermediate stages of synergid differentiation, well delineated, transparent areas were observed between the synergid cytoplasm and micropylar end wall (fig. 59). This

appearance during synergid differentiation suggests it may be an intermediate stage of synthesis in the formation of end wall ingrowths, although its non-polysaccharide nature is puzzling.

Egg cell — The egg is the largest cell of the egg apparatus. It is positioned chalazal to the two synergids, with a micropylar vacuole separating the egg nucleus and cytoplasm from the synergid-egg wall (fig. 50). Most often the single large vacuole tends to laterally displace egg cell cytoplasm (fig. 53). This polarity, whether the egg nucleus and cytoplasm are displaced to the side of the cell or the chalazal base, is characteristic of the egg. A PAS+ wall forms around the entire egg with no apparent thin areas where it contacts the central cell cytoplasm (fig. 53,54).

Nucellus

After sporogenous cells have differentiated, the nucellus forms a conical protuberance of the ovule primordium (fig. 1). Hypodermal and other vegetative cells separate sporogenous cells from the nucellar epidermis. No differences in ABB staining are found among vegetative nucellar cells, but within cells nuclei tend to be more ABB+ than the peripheral cytoplasm. Starch is found in the chalazal region of the nucellus. Ultrastructural information on ovules at the megasporocyte stage of development indicates that the surface wall of nucellar epidermal cells is thicker than the epidermal cell end walls, and has a thin layer of

electron dense material (fig. 5,6) which is probably a cuticular substance secreted by the epidermal cells. The inside wall of epidermal cells, separating the nucellar epidermis from hypodermal cells, tends to be thicker than epidermal cell end walls. Plasmodesmata appear to be restricted to the walls separating adjacent epidermal cells (fig.7).

During megasporogenesis, the nucellus undergoes approximately a twofold axial enlargement with the establishment of three morphologically and cytologically distinctive regions; the nucellar epidermis (fig. 12,14), micropylar vegetative cells (fig. 14), and chalazal vegetative cells (fig. 13). Cross walls of the nucellar epidermis are perpendicularly oriented. Cytoplasm of epidermal cells stains lightly with ABB and does not contain many conspicuous vacuoles. Micropylar epidermal cells contain numerous starch grains while chalazal epidermal cells contain little starch. Nuclei stain darkly with ABB and have an uneven outline giving them a granular morphology. Other vegetative cells in the micropylar half of the nucellus have nuclear and cytoplasmic properties similar to the epidermal cells, but are dissimilar in having oblique end walls. In the chalazal nucellus an axial core of cells tends to have perpendicular end walls and lightly ABB+ cytoplasm which contains a few small vacuoles (fig. 13). Because the parenchyma cells of the outer integument have large vacuoles with peripheral cytoplasm, an integument-nucellus interface is established by this time (fig. 13). No starch is found in chalazal nucellar cells.

Nucellar cells in each of the three regions undergo prominent changes at the onset of megagametogenesis. Walls of the nucellar epidermis become very thick and intensely PAS+ (fig. 18,20,23). This wall morphology clearly delimits the nucellar epidermis from the external integumentary and ~~internal~~ nucellar tissue. Epidermal cell cytoplasm stains lightly with ABB and contains small vacuoles. Nuclei are present, but they do not stain as intensely as during the megaspore stage, nor do they appear irregularly shaped. The gradient of starch observed earlier in the nucellar epidermis is not evident since chalazal epidermal cells appear to accumulate as much starch as micropylar epidermal cells. Other nucellar cells in the micropylar region of the ovule have walls which react strongly with PAS, but not to the extent of epidermal cells (fig. 18,20). Elongate cells with oblique end walls are very prominent, particularly along the lateral surfaces of the female gametophyte. This "stretched" morphology is probably due to distortion and compression by the expansion of the female gametophyte. Nuclei and cytoplasm have an ABB affinity similar to epidermal cells, but intracellular vacuoles are much larger and more abundant. Starch is no longer detectable in these cells.

Cells immediately chalazal to the two nucleate gametophyte have thick PAS+ walls with irregular inside surfaces (fig. 22). Very few vacuoles are present in these cells in which ABB+ nuclei occupy most of the volume. The extreme chalazal end of the nucellus consists of cells cytologically similar to those observed at the megaspore

stage. They are relatively thin walled and contain lightly ABB+ cytoplasm with numerous small vacuoles. Nuclei are slightly more ABB+ and tend to be elliptical. An intermediate zone of cells with its own peculiar characteristics separates the thin walled chalazal cells from the thick walled cells adjacent to the female gametophyte. Wall alteration in these cells appears to be in an incipient stage; numerous starch grains, not observed in other chalazal nucellar cells, are found.

Nucellar tissue continues to degenerate with the differentiation and expansion of a four nucleate coenocytic gametophyte (fig. 29, 30, 71). Most cell decomposition occurs at the micropylar end of the nucellus, extending radially outward from the gametophyte wall. Prior to the expansion of the four nucleate gametophyte, nucellar epidermal cells are intact and contain starch, while nucellar cells subjacent to the lateral and micropylar surface of the gametophyte wall are either crushed entirely or very distorted (fig. 30). Cells adjacent to the gametophyte wall usually have a homogeneous mass of very dense, ABB+ cytoplasm with no recognizable constituents. During the period of expansion of the four nucleate gametophyte, starch is mobilized from micropylar epidermal cells with the cells subsequently pressed against the inner integument. Chalazal epidermal cells are not distorted and retain thick walls and lightly ABB+ cytoplasm having few vacuoles (fig. 33). A similar organization of three zones in the chalazal nucellus exists as found earlier in ontogeny, but with larger deposits of

PAS+ wall material in cells near the chalazal base of the female gametophyte.

Longitudinal expansion of the eight nucleate gametophyte occurs at the expense of chalazal nucellar tissue (fig. 74) and remaining micropylar nucellar cells. In the chalazal nucellus, a tapering axial core of thick walled cells extends chalazally from the gametophyte (fig. 39). Starch filled hypodermal cells flank the axial core of degenerate nucellus while nucellar cells nearest the chalazal parenchyma contain little starch and remain thin walled with no indication of cell degeneration. When a mature embryo sac has differentiated from an eight nucleate coenocytic gametophyte, nearly all thick walled chalazal nucellar cells and lateral hypodermis are obliterated, leaving the embryo sac end wall adjacent to a residuum of thin walled nucellar cells (fig. 57,58). Remnants of nucellar cells separate the micropylar wall of the embryo sac from the inner epidermis of the outer integument (fig. 54,73). These cells consist of thin strands of ABB+ cytoplasm, PAS+ wall material, and a large amount of transparent material having no ABB or PAS affinity. No structural detail of thick nucellar walls could be resolved with light or electron microscopy. A broad electron-transparent area is present between adjacent degenerate nucellar cells (fig. 61). Electron dense inclusions, some of which appear to be membrane bound vesicles, are found in the wall. Cytoplasmic and nuclear material are loosely organized in the degenerative nucellar cells. Numerous membrane bound vesicles, few amyloplasts, and extensive rough endoplasmic

reticulum profiles are typically present (fig. 62,63).

Integuments

The garden pea ovule is bitegmic. Integument differentiation and enlargement during megasporogenesis and megagametogenesis results in the formation of a campylotropous ovule curved towards the apex of the carpel. Histologically similar primordia are initiated at megasporocyte differentiation (fig. 2) although subsequent development of the two integuments is radically different.

Inner integument — The inner integument is initiated by periclinal divisions of two adjacent rows of epidermal cells encircling the base of the nucellus (fig. 2,10). The integument primordium is organized into a bilayer of cytologically similar cells (fig. 3,69) with the integument-nucellus junction marked by a meandering, branched layer of electron dense material on the surface walls of epidermal cells (fig. 11). This layer, interpreted as a cuticle, is continuous with the electron dense layer of the nucellar epidermis and the funicular epidermis. At the completion of megasporogenesis, the integument primordium has advanced to half the length of the nucellus, placing the integument apex along a radius which intercepts the functional megaspore (fig. 12). Growth is restricted to anticlinal divisions and axial enlargement such that the integument consists of a bilayer of cells growing intrusively between the nucellus and outer integument. Cells of the inner integument have thin, PAS+ walls, ABB+ cytoplasm and nuclei, and scattered traces of small starch grains (fig. 12). When

a two nucleate gametophyte is present and in succeeding stages, the apical rim of the inner integument terminates shortly before the micropylar apex of the nucellus, forming a relatively broad endostomal pore (fig. 18,29). Expansion occurs along the lateral surface of the integument by periclinal divisions, but generally not more than 3-4 cell layers (fig. 23). An exception is the micropylar region of the integument where cells proliferate forming a swollen apical zone (fig. 29). This area fills any free space between the nucellus and outer integument, excepting the wide endostome, where nucellus or gametophyte lie in close proximity to the outer integument. Starch accumulates in most cells of the integument during megagametogenesis, although a polarized micropylar concentration is found when a mature embryo sac is present (fig. 42-44).

The interface of the inner and outer integuments is bordered by a thin cuticle which appears to be partly derived from each integument (fig. 56,64). The cuticle covering the inside surface of the inner integument is considerably thicker and apparently derived entirely from the integumentary epidermis (fig. 67). Two different areas in this latter cuticle could be resolved. The inner half adjacent to the integument cell wall consists of electron dense blebs, while the surface material adjacent to the nucellar cells consists of alternating strands of electron dense and electron transparent material. No plasmodesmata are found in epidermal walls of either surface, although they are fairly common in other walls within the integument.

Outer Integument—The outer integument is initiated a few cells chalazal to the inner integument (fig. 2). Eccentric growth of the dorsal half results in the curvature of the ovule towards the style, while the ventral half remains relatively undifferentiated. Growth of the dorsal half of the outer integument during megasporogenesis brings its inner epidermis adjacent to the nucellar epidermis, indicating a more rapid rate of growth relative to the inner integument (fig. 12). Differential growth of the outer integument continues such that its basic morphological organization is completed during early megagametogenesis with the enclosure of the inner integument, nucellus, and female gametophyte. Subsequent differentiation, most of which is restricted to the dorsal segment, involves mitotic activity and cell enlargement which broadens and lengthens the integument. The chalazal base of the dorsal region consists of obliquely oriented packets of 4-7 cells within a histological sector radiating from the chalazal base of the nucellus to the terminus of the vascular strand (fig. 38). Inner epidermal cells which border the inner integument divide periclinally forming a stratified margin (fig. 44). A notable exception occurs in a ventral group of epidermal derivatives below the ventral arch of the embryo sac (fig. 44). In the post fertilization enlargement of the ovule, these cells and their derivatives form the ovular basal body, a group of parenchymatous cells extending into the arch of the enlarged embryo sac (Bocquet 1959).

The exostomal component of the micropyle is a slit-like

entranceway aligned parallel to the long axis of the ovary. It is not formed by apical growth of the extreme dorsal surface of integumentary tissue, but by the proliferation of terminal and subterminal cells between the dorsal and ventral segments of the integument (fig. 28,31). These cells divide periclinally and subsequently enlarge to fill in any exostomal gaps by forming lateral flanges of integumentary tissue.

Starch in the outer integument is localized at the chalazal base of integumentary tissue during megasporogenesis with a large distribution of starch reserves between the terminus of the vascular tissue and the chalazal base of the nucellus. The amount of starch, particularly in this region, increases commensurate with the development of the ovule. During differentiation of the eight nucleate coenocytic gametophyte into a mature embryo sac, starch also accumulates in a decreasing gradient towards the micropylar region of the integument.

Vasculature — The ovule of Pisum has a single vascular strand which extends through the funiculus into the dorsal segment of the outer integument (fig. 38). The entire strand increases in width and length with the development of the ovule. Xylem and phloem differentiation is initiated during megagametogenesis, although maturation prior to fertilization and subsequent ovule enlargement is minimal.

Cytohological zonation is apparent at the megaspore mother cell stage (fig. 4) with a strand of elongate cells differentiating from peripheral vacuolate cells. This strand

of procambial tissue is continuous with the placental vasculature and extends into the ovule to the chalaza. Procambial cells within the ovule primordium are densely ABB+ and contain few vacuoles while those of the placental trace (between the base of the funiculus and placental vasculature) tend to be more vacuolate. When four megaspores are present in the ovule, cells in the outer integument have differentiated into procambium such that the vascular strand terminates midway into the dorsal segment (fig. 15,16). Procambial cells in the placental trace and ovule vascular strand are cytologically similar to the procambium described above.

Vascular differentiation is initiated in the ovule during the two and four nucleate stages of megagametogenesis. Procambial cells, particularly those at the inner margin of the vascular strand, become increasingly elongate (fig. 24, 25, 32, 34). Most cells also become highly vacuolate early in gametogenesis. The pattern of xylem and phloem maturation is evident during the differentiation of the eight nucleate coenocytic gametophyte into a mature embryo sac (fig. 38, 40, 65, 66). Sieve tube elements appear near the outer edge of the vascular strand, whereas tracheary maturation occurs near the inner edge (fig. 65, 68). Within the ovule, initial maturation of xylem and phloem begins midway along the vascular strand. Subsequent maturation of sieve tube elements proceeds basipetally, but the presence of immature xylem elements at the same level as mature sieve tubes in the funiculus indicates that xylem maturation may be slower.

No acropetal maturation of xylem or phloem could be detected prior to fertilization.

Discussion

The Polygonum type of megasporogenesis and megagametogenesis observed in this study of Pisum concurs with the earlier observations of G.O. Cooper (1938). The number of sporogenous cells which differentiate in the nucellus is not generally agreed upon for Pisum. In an investigation of several members of the Leguminosae, including *P. sativum*, Roy (1933) concluded that the archesporial cell functions directly as the megaspore mother cell. G.O. Cooper (1938) observed that the archesporial cell divided to form a primary parietal cell in the hypodermis and a primary sporogenous cell embedded in the nucellus. Although the sequence of sporogenous cell derivation was not examined in this study, it is likely that an archesporial cell divides prior to differentiating into a sporogenous cell because of the location of sporogenous cells within the hypodermal layer. An alternative derivation of a crassinucellate ovule would be by repeated periclinal divisions of epidermal cells which would subsequently position sporogenous cells deep within the nucellus (Maheshwari 1950), but no evidence of this pattern of development was found.

That synthetic activity in the megaspore mother cell may be restricted within the nucleus is suggested by the lightly ABB+ megaspore cytoplasm and the darkly ABB+ nucleolus in the megasporocyte nucleus. In a light microscope study of sunflower megasporogenesis Newcomb (1972) also found that the megaspore mother cell appeared less dense than surrounding cells and contained a prominent

nucleolus, but apparently without any peculiar morphological characteristics such as those reported here for Pisum. Also, few organelles related to synthetic activities were observed in the megasporocyte cytoplasm of sunflower, whereby Newcomb suggested that the megasporocyte is specialized for nucleic acid synthesis and not cytoplasmic synthesis. The intense ABB+ reactivity of the megasporocyte nucleolus in Pisum indicates a large amount of protein in the nucleolar volume, although whether this represents protein synthesized in the nucleolus, and/or a high concentration of enzymes associated with RNA synthesis could not be determined. Protein synthesis within the nucleolus has been well documented for animal and plant cells (see DuPraw 1968 and references therein). Sirlin (1960) demonstrated that H^3 -leucine is uniformly incorporated throughout nuclei of chironomid salivary cells. Working with pea seedlings, Birnstiel et al (1962) found that the nuclear accumulation of tritiated leucine was restricted to the nucleolus at first and that only later did labelled protein appear in the chromatin. Their suggestion that the nucleolus may export protein to the chromatin was supported by later work (Birnstiel and Flamm 1964) where some of the proteins synthesized in pea seedling and tobacco nucleoli were found to be histone and non-histone basic proteins. It is interesting that the first appearance of the nucleolus in the megasporocyte of Pisum occurs when the nucleoplasm is relatively homogeneous and translucent. Subsequently, darkly ABB+ material appears in the nucleoplasm in addition

to the distinctive nucleolus. While there is little doubt that the ABB+ material in the nucleoplasm is protein, it is tempting to speculate that it consists of histones previously synthesized in the nucleolus.

Soon after the four megaspores have differentiated, the chalazal megaspore begins to enlarge with the concomitant degeneration of other megaspores. The transient persistence of the megaspore adjacent to the functional megaspore has not been previously noted for the Polygonum type of development. Since the megaspore expands toward the micropyle during gametogenesis (see fig.74) it is interesting that the adjacent megaspore, unlike the micropylar megaspores should persist if only for a short period of time. This indicates that non-functional megaspore degeneration is not an all or none response to the encroaching gametophyte, and probably is a regulated process of cell degradation by which the gametophyte could derive nutrients during its earliest development.

The female gametophyte remains coenocytic during the two, four, and early eight nucleate stages of development. Transition into a seven celled embryo sac would seem to require the segregation of cytoplasm, cell membrane formation, deposition of wall material and any subsequent intracellular differentiation. The temporal relationships of these events to the last mitotic division and the mechanisms involved have not received a great deal of attention, even though a free nuclear stage preceding the formation of a cellular embryo sac is characteristic of all angiosperms which have

been investigated (see Maheshwari 1950).

In *Lilium henryi*, wall formation is associated with the spindle apparatus of the last set of mitotic divisions (Cooper 1935). This mechanism of wall formation is probably similar to that found in somatic cells involving cell plate formation in the equatorial plane of a phragmoplast, and subsequent deposition of wall material (see Esau 1965). In *Pisum*, however, the presence of eight nuclei not bound by any wall material indicates that wall formation is not associated with the spindle apparatus of the third set of mitotic divisions. Newcomb (1972) suggested antipodal walls in sunflower are freely formed because of the occurrence of incomplete walls found at the chalazal end of the embryo sac. It was presumed walls were growing at the time of fixation by vesicles produced by dictyosomes near the tips of the free walls. Synthesis of new wall material at the end of a free wall projecting into the embryo sac is difficult to visualize when complete and relatively straight walls are produced in the antipodals as well as the egg apparatus. It seems reasonable that a mechanism to regulate the direction of wall synthesis may be a fundamental component for free wall synthesis during transition of the coenocytic gametophyte. Embryo sac free wall synthesis would then be distinguished from other types as in sunflower endosperm where free walls meander through the cytoplasm (Newcomb 1972).

The functional significance of antipodal cells as they relate to embryo sac nutrition is unclear because of the difficulty associated with obtaining data on the specific

timing of cell formation and degradation. The transient occurrence of antipodal cells and their small size is not suggestive of cells having an important role in embryo sac nutrition although a temporary role in embryo sac expansion may be associated with them. During the transition of the eight nucleate gametophyte into an embryo sac the chalazal end of the gametophyte expands and replaces degenerative nucellar cells (see fig. 74). However, more information about the differentiation and degradation of antipodal cells is required to establish a firm correlation.

The three-celled egg apparatus is morphologically similar to that found in many angiosperms (see Maheshwari 1948, 1950). Noteworthy are the synergid wall ingrowths which have not been previously documented for Pisum sativum. The participation of synergid cells in the transfer of nutrients into the embryo sac via the wall ingrowths is unlikely for a number of reasons. Synergid wall ingrowths form concurrent with the differentiation of other cells within the embryo sac, and consequently they could only facilitate nutrient entry after the formation of a mature embryo sac. By this time, however, most nucellar tissue adjacent to the micropylar end wall of the synergids has degenerated leaving only thin strands of densely ABB+ cytoplasm indicating that the bulk of any resorption of nucellar tissue which may occur would have been accomplished prior to synergid cell differentiation. The location of synergids at the micropylar end of the megagametophyte is positionally favorable to the uptake of nutrients from the

outer integument, but no cytological or histological evidence was found in outer integument cells to strongly suggest this as a route of nutrient flux to the embryo sac.

Degradative developmental changes in the nucellus are correlated with megagametophyte ontogeny and indicate that nucellar cell breakdown is not a random event. During the coenocytic and cellular stages of megagametogenesis, megagametophyte expansion is directed toward the micropylar end of the nucellus (see fig. 74), while chalazal expansion is restricted to the period of gametophytic differentiation into a cellular embryo sac. Nucellar cell degradation is characterized by sequential cytological alterations which occur as follows:

1. intense PAS+ wall thickening
2. starch mobilization
3. wall degradation (loss of intense PAS+) but retention of structural framework
4. densely ABB+ protoplasts
5. obliteration of nucellar cell structural integrity by the expanding gametophyte.

An interesting aspect of nucellar degradation is the sequential mobilization of starch in the micropylar nucellus. Cells within the nucellar epidermis contain starch which is mobilized prior to expansion of the gametophyte. These cells then go through the remaining cytological changes given above. Within the nucellar epidermis, however, only wall thickening is concurrent with the wall alteration of other micropylar nucellar cells. Starch mobilization and subsequent degrad-

ative events within the nucellar epidermis do not proceed until the gametophyte wall is in close proximity to the inside wall of the nucellar epidermis.

Even more striking is the delay in the degradation of chalazal nucellar cells near the base of the female gametophyte. These cells undergo wall thickening early in gametogenesis, but do not complete subsequent stages of degradation until the eight nucleate coenocytic gametophyte differentiates into a cellular embryo sac. The irregular wall morphology of these cells suggests they may be comparable to so called "transfer cells" which have been implicated as intermediary structures involved in short distance solute transport (Gunning et al 1968; Gunning and Pate 1969; Pate and Gunning 1969, 1972; Pate et al 1970). The timing of their formation, coincident with gametogenesis, may be a response to increased solute flux into the megagametophyte from a chalazal route of entry. Pate et al (1970) provide evidence that wall ingrowth formation in transfer cells is suppressed where solute flow is reduced, but capable of being reestablished after the applied stress is removed. The possibility exists, however, that irregular wall formation is not a response to increased nutrient flux, but simply a cytological peculiarity of chalazal nucellus degradation. While transfer cells have been found in structurally diverse plant organs (see Pate and Gunning 1972), they have not previously been implicated as part of a degenerative process. Moreover, the randomness of wall irregularities in degenerate chalazal nucellus is in marked

42

contrast to the polarized formation of wall-ingrowths in transfer cells (see Pate et al 1970).

The cytological changes and temporal aspects of nucellar cell degradation raise questions about the controlling mechanism(s) of cell degradation and encroachment by the gametophyte. In the micropylar nucellus, what features of nucellar epidermal cells allow the postponement of starch mobilization until the megagametophyte is in close proximity to the epidermal wall? How are cytological changes brought about which closely correlate with megagametophytic expansion? How is the selective degradation of nucellar tissue controlled? It is interesting to speculate that the megagametophyte may regulate nucellar degradation in the course of its expansion, possibly by a hormonal-based mechanism which could induce one or a combination of steps in the sequence of degradative events. Hormonal interaction in the nutrition of a plant system which induces lytic activity in a histologically distinctive tissue is not without precedent. Stimulation of α -amylase synthesis in barley aleurone layers by gibberellin secreted by the embryo is well established (Paleg 1960, 1965; Varner 1964; Varner and Chandra 1964; Jacobsen and Varner 1967). Newly synthesized α -amylase and other hydrolytic enzymes are secreted into the endosperm and act on starch in the cells converting it to sugar used by the developing embryo.

Nutrient influx into the ovule probably occurs by different mechanisms dependent on the developmental age

0

of the ovule. The absence of a procambial strand in the ovule prior to megasporocyte differentiation indicates that nutrients entering the ovule primordium may not follow a localized route. The small size of the ovule would be amenable to nutrient flux by a diffusion mechanism because of the relatively short distance involved. Diffusion over distances less than 100 μm is relatively rapid (ca 0.6 sec.) and may be enhanced by cytoplasmic streaming (Nobel 1974). In an older ovule where diffusion alone would be an inefficient mechanism for nutrient flux, the establishment of a vascular strand in the ovule would provide a restricted and presumably more efficient translocation pathway. However, the immature condition of most vascular tissue in the ovule prior to fertilization raises the interesting question if procambial or differentiating vascular tissue has the capacity to translocate mineral and organic nutrients. Although a voluminous literature exists on translocation in plants, information related to movement in undifferentiated vasculature is fragmentary. Experiments on lateral bud development following stem decapitation in Pisum sativum indicated that C-14 photosynthate is translocated to the developing lateral bud in restricted pathways well before phloem maturation (Wardlaw and Mortimer 1970). Before a lateral bud was released from inhibition by stem decapitation, Wardlaw and Mortimer observed that a procambial trace connected the bud to the vasculature of the stem. Autoradiographs of C-14 labelled photosynthate translocated into the bud at this stage and

up to 24 hrs. after decapitation showed a diffuse distribution of radioisotope indicating the lack of a well-defined conducting system. About 24 hrs. after release of inhibition, procambial cells showed some expansion and orientation with a decrease in staining intensity, but no complete phloic differentiation for 4-5 days. The degree of vascular differentiation was correlated with a localized pathway and increased rate of uptake over the 4 day period until a maximum was reached shortly after 5 days when mature sieve elements were present. It is noteworthy that vascular differentiation in the garden pea ovule begins during or shortly after the onset of megagametogenesis. If a mode of translocation similar to the one found by Wardlaw and Mortimer in lateral bud development operates in the ovule, it would suggest that an increased flow of metabolites into the ovule via a localized pathway is initiated concurrent with megagametogenesis. Moreover, as the ovule enlarges during megagametogenesis it would presumably require additional nutrients which could be obtained since the rate of translocation into the ovule would be continually increasing as the differentiating vascular tissue approaches maturity.

The presumed flux of nutrients to the embryo sac has been suggested to occur via an integumentary or chalazal route of nutrient entry (see Fig. 75). The integumentary route proposed by Linskens (1969) may be a direct route involving the shortest distance between the terminus of the vascular strand and megagametophyte, or alternatively nutrients could enter the chalazal base of the integument

and then be transferred to the megagametophyte through the inside wall of the integument. However, both of these integumentary pathways appear unlikely for a number of considerations. No cytological evidence was found to suggest a direct flow of nutrients to the embryo sac by the shortest possible route to the megagametophyte. This mode of nutrition would require nutrient flux through the inner integument-outer integument interface, but the absence of plasmodesmata in adjacent walls and the electron dense surface material seem to be more of a barrier than passageway to the flow of nutrients. Similarly, the thick electron dense material on the inside wall of the inner integument may prevent catabolic changes in integumentary cells during nucellar degradation, hence maintaining a physiological discontinuity between the inner integument and megagametophyte. That the inner integument may be physiologically independent of interaction with the megagametophyte is suggested by the polarized accumulation of starch during megagametogenesis, similar to the polarized accumulation of starch in the nucellar epidermis during megasporogenesis. Post-fertilization changes in the inner integument indicate that it is functionally associated with embryonic rather than embryo sac nutrition, where embryo sac expansion following fertilization is closely correlated to starch mobilization and selective degradation of inner integument cells.

Nutrient influx via a chalazal route would necessitate translocation through integumentary parenchyma between the

chalazal base of the nucellus and the terminus of the vascular strand. The chalazal sector of oblique cell packets histologically corresponds to this zone of cells (see Fig. 38). The consistent presence of starch in these cells and their approximate parallel alignment with the most direct route between the chalaza and vascular terminus suggest they may participate in a localized rather than diffuse movement of solutes from the vascular terminus to the chalaza. Movement of solutes in the chalazal nucellar cells may be facilitated by the elongate morphology of these cells, although it is difficult to conceive a mechanism by which solutes are subsequently transferred through degenerate nucellar cells before reaching the megagametophyte.

The proposal of a chalazal or integumentary route of nutrient transport to the embryo sac presumes direct involvement of the parent sporophyte in megagametophyte nutrition. In Pisum, however, degenerative nucellar tissue may provide most and perhaps all nutrients required by the gametophyte during megagametogenesis. Degenerate wall material and starch accumulated in the nucellus could be mobilized as sugar sources for the developing gametophyte, while protein, nucleic acid, and lipid precursors may be derived from degenerating cytoplasm. That adequate nutrients may be available in the nucellus is suggested by the persistence of a chalazal residuum of nucellar tissue near the base of the mature embryo sac. During megagametogenesis a mitotic step always preceded an increase in gametophyte

volume. The associated gametophyte wall expansion could serve the dual function of placing the megagametophyte in close proximity to additional reserves (e.g. in the nucellar epidermis) while substantially increasing the total surface area to facilitate nutrient absorption. Self maintenance of this kind is an interesting alternative to formerly proposed modes of embryo sac nutrition, but it is recognized that experimental evidence of the kinetics, quality, and quantity of nutrient flux in the ovule during megagametogenesis is required before a conclusive statement is made regarding the mechanism(s) of embryo sac nutrition.

List of abbreviations used for all micrographs: Ant = antipodals; CC = central cell; CCC = central cell cytoplasm; Cha = chalaza; CN = chalazal nucellus; D = dictyosome; DM = degenerate megaspores; DN = degenerate nucellus; E = egg; EA = egg apparatus; Ep = epidermis (nucellar); ESW = embryo sac wall; FM = functional megaspore; Fu = funiculus; G = gametophyte; Hy = hypodermis; II = inner integument; Mic = micropyle; MMC = megasporocyte (megaspore mother cell); NCW = nucellus cell wall(s); Nu = nucleus; Nuc = nucellus; Nucl = nucleolus; OI = outer integument; Pc = procambium; Pd = plasmodesmata; PN = polar nuclei; RER = rough endoplasmic reticulum; S = starch; Sp = sporogenous cells; Syn = synergid cell; V = vasculature.

Fig. 1. Light micrograph of ovule primordium. Sporogenous cells (Sp) are within the hypodermis of the nucellus. A few starch grains (arrow) are present at the site of integument initiation. Brightfield. X 752.

Fig. 2. Light micrograph of young ovule with a differentiated megasporocyte (MMC). A densely ABB+ nucleolus (small arrow) is found in the megasporocyte nucleus. Integument primordia (large arrows) differentiate from the epidermis and appear as small outgrowths on the surface. Starch is found at the chalazal end of the nucellus and also in the nucellar epidermis. Phase contrast. X 752.

Fig. 3. Light micrograph of nucellus with a megasporocyte (MMC) at early prophase. Note the presence of a vacuolate nucleolus in the MMC nucleus. A line representing the nuclear membrane of the megasporocyte is clearly seen with the light microscope during early meiotic prophase. Inner integument primordia form a cup-like bilayer of cells surrounding the nucellus. Phase contrast. X 768.

Fig. 4. Light micrograph of ovule vasculature when a megaspore mother cell has differentiated in the nucellus. The procambium (Pc) consists of a strand of elongate cells continuous with the ovary vasculature and terminating at the chalaza. Numerous mitotic figures (arrows) occur in the procambial trace. Phase contrast. X 440.

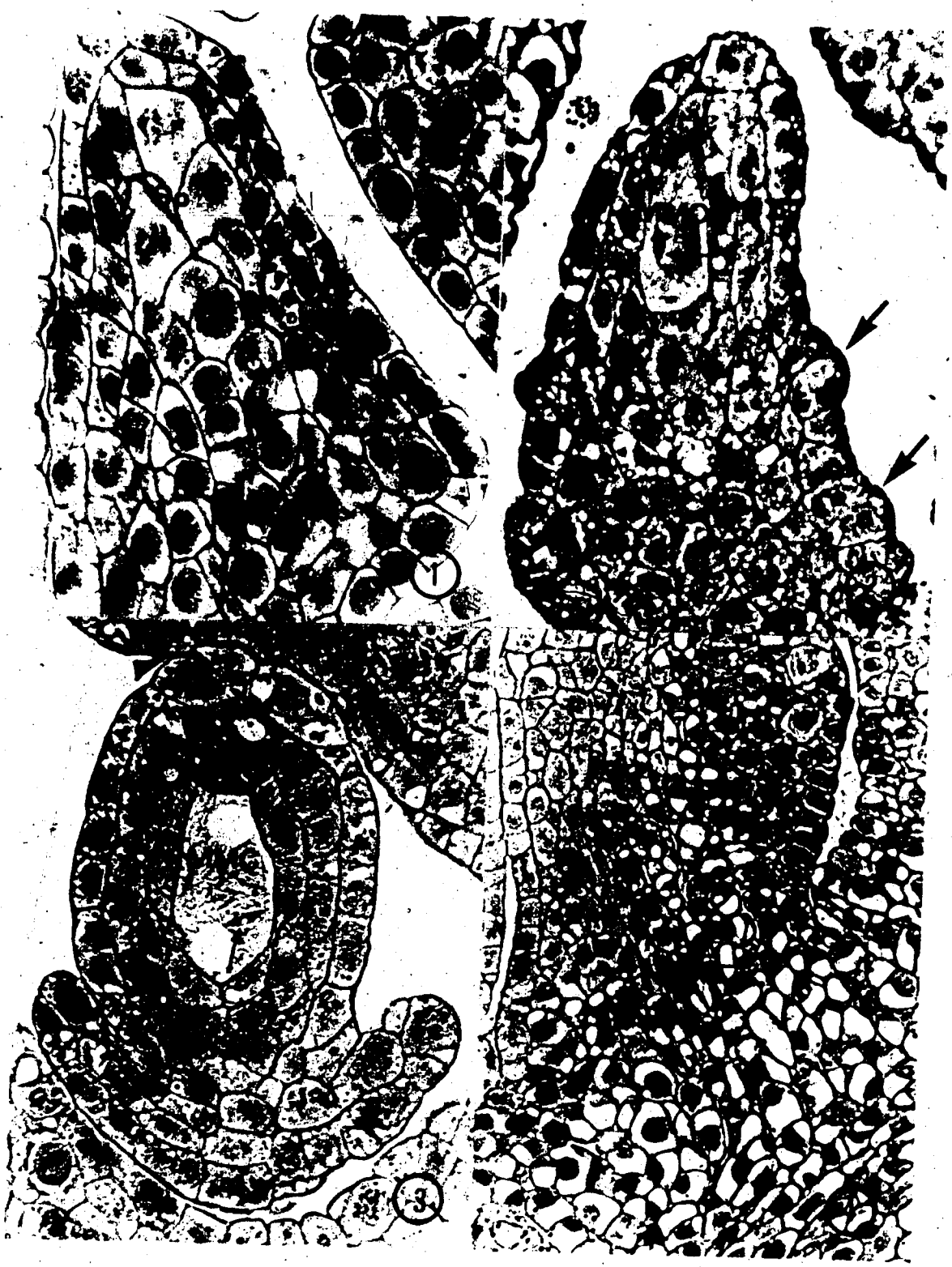


Fig. 5. Electron micrograph of nucellar epidermal (Ep) and hypodermal (Hy) cells. Hypodermal cells have thin walls except for the relatively thick wall separating them from the epidermis. Most cells have very few vacuoles with the majority of cell volume occupied by large nuclei. X 4,340.

Fig. 6. Electron micrograph of surface detail of the nucellar epidermis. The surface wall (arrows) is coated with an electron dense layer of material. Note the rough contour of the surface wall. X 4340.

Fig. 7. Electron micrograph of plasmodesmata in contiguous walls of nucellar epidermal cells. Plasmodesmata were rarely observed in the inside wall between the epidermis and hypodermis. X 31,000.

Fig. 8. Light micrograph of enlarging chalazal megaspore (FM) of a T-shaped tetrad. The adjacent megaspore does not degenerate at the same time as the two micropylar megaspores (arrows). Brightfield. X 1,000.

Fig. 9. Light micrograph of enlarging megaspore cytoplasm. Granular inclusions (arrows) stain lightly with ABB. Other smaller rod-shaped particles in the cytoplasm stained darkly with ABB. The nucleus (Nu) is located at the micropylar end of the cell near the degenerating megaspores (DM). Phase contrast. X 950.

Fig. 10. Electron micrograph of inner integument primordium. Two epidermal cells have divided periclinally to form the integument initials which protrude from the surface of the ovule. Thin walls (arrows) separate the daughter cells. One of the outer derivatives has divided periclinally, forming a three-tiered primordium (upper part of photograph). X 3,100.

Fig. 11. Electron micrograph of inner integument-nucellus junction. A thin electron dense layer of surface material covers the surface of the integument (II) and nucellar (Nuc) epidermis. X 16,700.



Fig. 12. Light micrograph of ovule with four megaspores. The inner integument (II), a bilayer of cells, has advanced to half the length of the nucellus (Nuc). The apex of the dorsal segment of the outer integument (OI) has grown beyond the inner integument placing it in contact with the nucellar epidermis. Brightfield. X 307.

Fig. 13. Light micrograph of chalazal nucellus of an ovule with four megaspores. Vacuolate cells at the chalaza (Ch) form a histological junction with chalazal nucellar cells. Brightfield. X 1,108.

Fig. 14. Light micrograph of micropylar region of nucellus with four megaspores. The chalazal megaspore (FM) is the largest of the four. Note the accumulation of starch in the nucellar epidermis and smaller starch grains in hypodermal cells. Brightfield. X 1,150.

Fig. 15. Light micrograph of procambial (Pc) strand in the ovule at the four megaspore stage of development. The strand extends beyond the chalaza and terminates in the dorsal part of the outer integument. Procambial cells contain vacuoles and tend to be densely cytoplasmic. Brightfield. X 440.

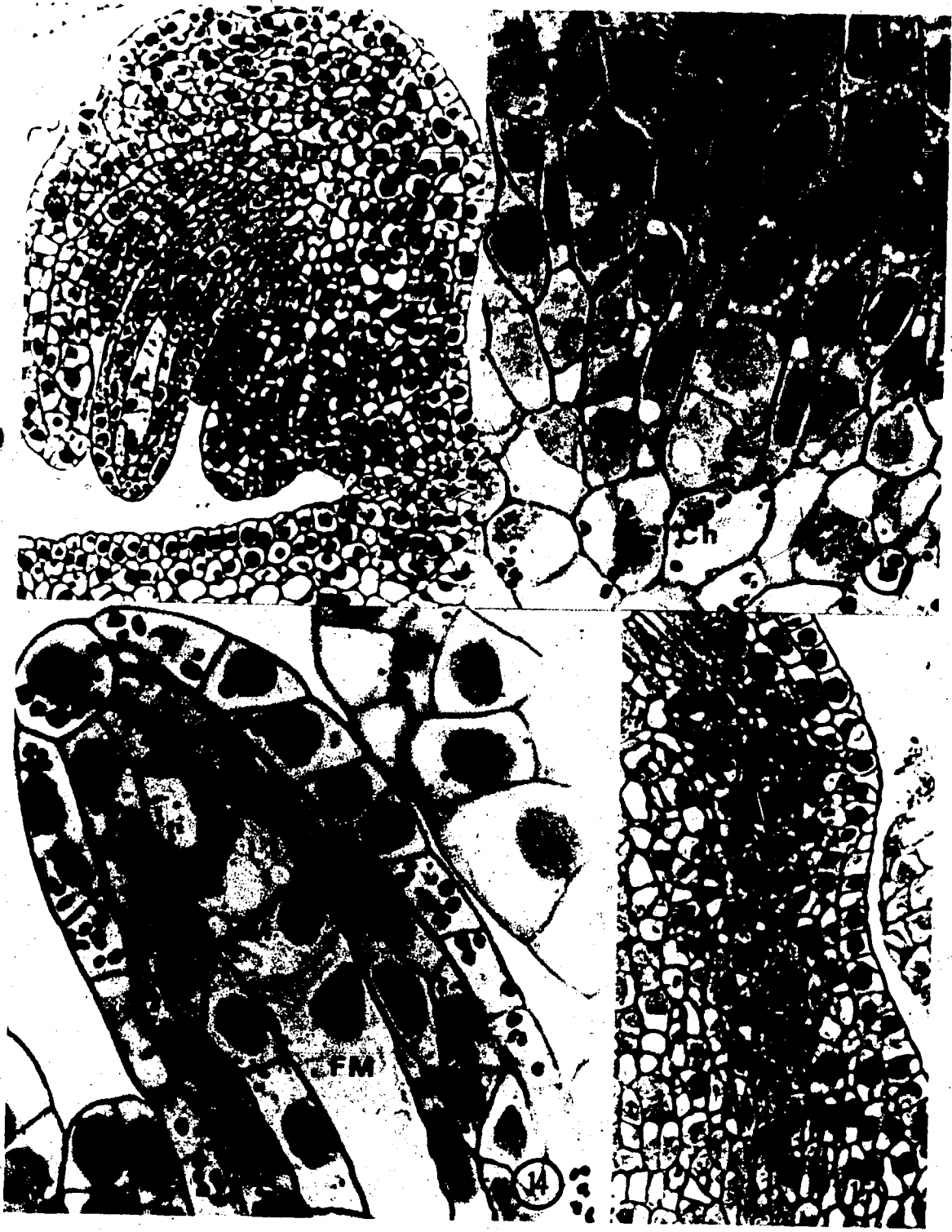


Fig. 16. Light micrograph of funicular procambium at four megaspore stage. The procambial cells (Pc) between the base of the funiculus and the placental strand are more vacuolate than those within the ovule. Note the mitotic figures in the cells (arrows). Phase contrast. X 430.

Fig. 17. Light micrograph of two nucleate gametophyte. The two nuclei of the gametophyte are prominent, but it is difficult to evaluate the cytological condition of the nucellar cells and the adjacent inner integument. Paraffin embedded. Brightfield. X 440.

Fig. 18. Light micrograph of young two nucleate gametophyte (G) prior to migration of nuclei to the chalazal and micropylar poles. Walls of the nucellar epidermis stain darkly with PAS. Note the extension of the inner integument (II) near the apex of the nucellus. Starch is beginning to accumulate in the outer integument. Brightfield. X 450.

Fig. 19. Light micrograph of two nucleate gametophyte (G) after vacuole formation. Note the degenerate megaspores adjacent to the expanding gametophyte (arrow). Paraffin embedded. Brightfield. X 680.

Fig. 20. Light micrograph of two nucleate gametophyte after vacuolation. The black material at the micropylar end of the gametophyte is the remaining darkly ABB+ protoplasm of degenerate megaspores. Nucellar epidermal cells have darkly PAS+ walls in the micropylar half of the nucellus. Thick walled nucellar cells are also apparent near the chalazal wall of the gametophyte. Note the retention of starch in the nucellar epidermis, and the absence of starch in other micropylar nucellar cells. Brightfield. X 680.

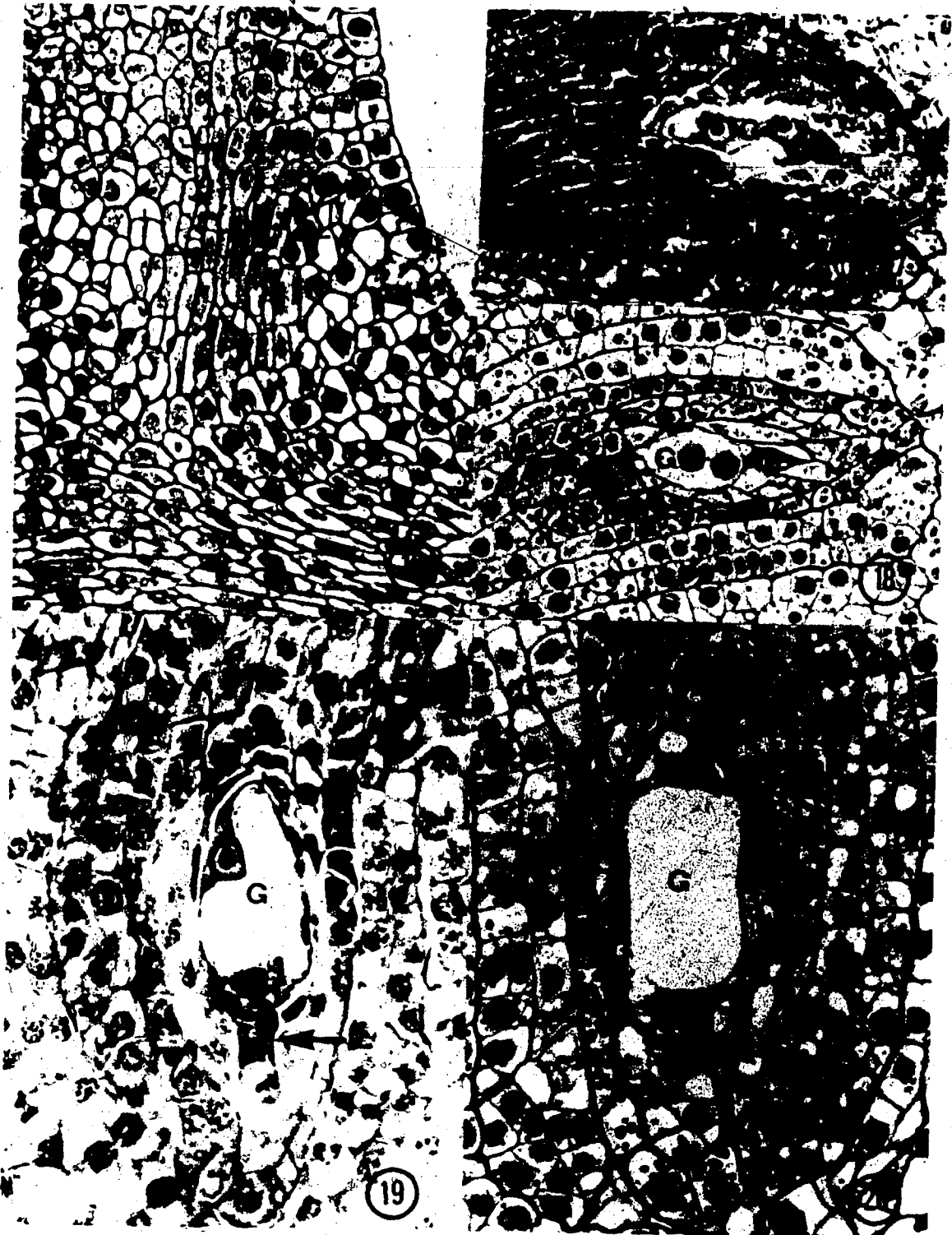


Fig. 21. Light micrograph of entire ovule with two nucleate gametophyte. The gametophyte (G) is embedded in degenerate nucellar tissue (Nuc) with darkly stained walls. The inner (II) and outer (OI) integuments invest the nucellus. Note the curvature of the ovule, placing the micropyle in close proximity to the inside wall of the ovary. Brightfield. X 275.

Fig. 22. Light micrograph of chalazal nucellus in a two nucleate gametophyte. Darkly stained PAS+ walls with irregular inside surfaces (arrows) form in cells near the base of the megagametophyte.

Fig. 23. Light micrograph of chalazal nucellus in a two nucleate gametophyte. The megagametophyte is eccentrically positioned in degenerating nucellar (Nuc) tissue. Starch laden nucellar epidermal cells demarcate nucellar tissue from the inside wall of the inner integument (II). Note periclinal divisions in a few of the integumentary cells. Transverse section. Brightfield. X 540.

Fig. 24. Light micrograph of ovule vasculature at the two nucleate gametophyte stage. Procambial cells (Pc) become vacuolate and elongate at the onset of megagametogenesis although no mature vascular tissue is found. The vascular strand ends abruptly in the dorsal segment of the outer integument (arrows). Brightfield. X 275.

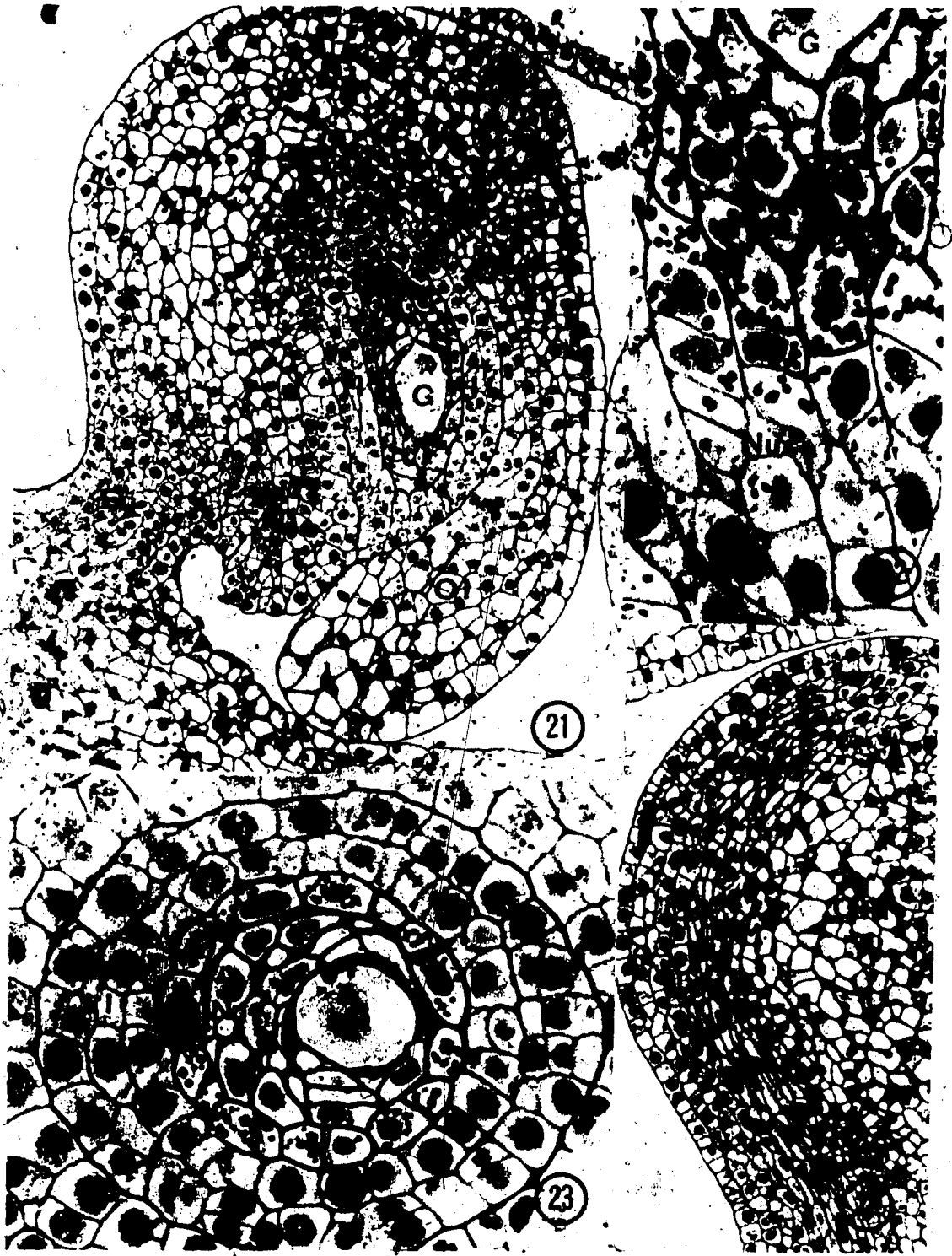


Fig. 25. Light micrograph of funicular procambium at the two nucleate gametophyte stage. Funicular procambial (Pc) cells are brick shaped and not as elongate as procambial cells in the ovule. Brightfield. X 280.

Fig. 26. Light micrograph of micropylar cytoplasm in a four nucleate gametophyte (G). Small vacuoles are present in the polar accumulation of cytoplasm. The nucleus contains a densely ABB+ nucleolus and scattered areas of heterochromatin. Brightfield. X 882.

Fig. 27. Light micrograph of four nucleate gametophyte and inner integument. Only the pair of micropylar nuclei were obtained in this section. Note the difficulty in assessing cytological differences between nucellar and integumentary cells. Paraffin embedded. Brightfield. X 310.

Fig. 28. Light micrograph of transverse section through micropyle. Mitotic figures in apical and subapical cells (arrows) of lateral flaps of integumentary tissue divide periclinal and form a tight micropylar pore (Mic). Brightfield. X 882.

Fig. 29. Light micrograph of early four nucleate gametophyte, nucellus, and inner integument. At the four nucleate stage, two nuclei are found at each pole of the megagametophyte. Note how the inner integument does not completely invest the micropylar tip of the nucellus (upper part of photograph). Brightfield. X 540.

Fig. 30. Light micrograph of late four nucleate gametophyte, nucellus, and inner integument. Soon before nuclei of the four nucleate gametophyte divide, the megagametophyte (G) has displaced most of the micropylar nucellus leaving remnants of darkly ABB+ nucellar cells. Arrows point to thick, but lightly PAS+ walls of degenerate nucellar cells. Note that the entire nucellar epidermis along the lateral surface of the megagametophyte has not degraded. Brightfield. X 560.



Fig. 31. Light micrograph of micropylar slit formed by the outer integument.. The slit like pore tapers from the locule of the ovary to the egg apparatus. The inner integument does not form a histological barrier at the inner opening of the endostome. Brightfield. X 340.

Fig. 32. Light micrograph of funicular vasculature in ovule at the four nucleate gametophyte stage. Procambial cells retain a brick-shaped morphology. Mitotic activity is evident (arrow). Brightfield. X 350.

Fig. 33. Light micrograph of chalazal nucellus at the late four nucleate gametophyte stage. Note the irregularly thickened walls (arrows) of cells near the chalazal base of the megagametophyte. A histological organization similar to the two nucleate stage is evident (see Fig. 23). Brightfield. X 856.

Fig. 34. Light micrograph of ovule vasculature at four nucleate gametophyte stage. Differentiating cells become increasingly elongate, but no mature xylem or phloem was observed. Brightfield. X 350. ✓

Fig. 35. Light micrograph of ovule at eight nucleate gametophyte stage. The micropylar wall of the megagametophyte is separated from the inner surface of the outer integument by a few remnant nucellar cells (arrow). The inner integument tends to have darkly ABB+ cells and a micropylar accumulation of starch. A broad outer integument (OI) of mostly vacuolate cells invests the gametophyte, nucellus, and inner integument. Brightfield. X 198.

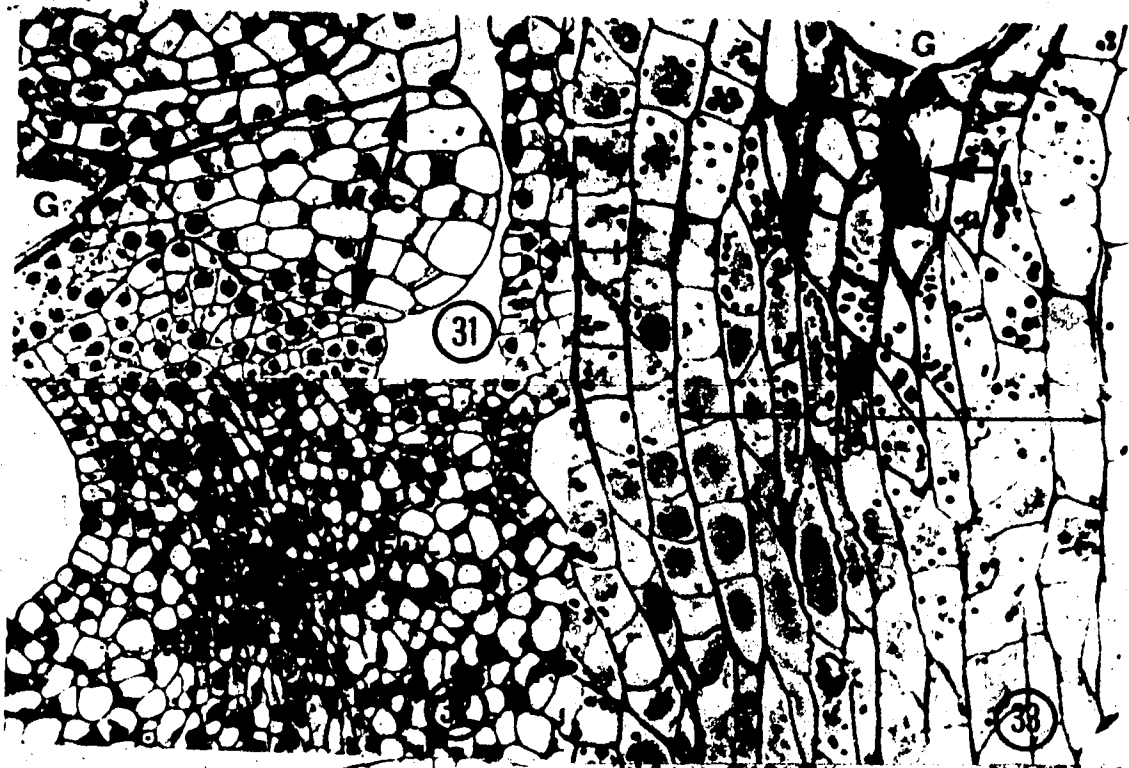


Fig. 36. Light micrograph of chalazal cytoplasm of an eight-nucleate gametophyte. Small vacuoles occur in the cytoplasm. Note the degenerate chalazal nucellar cells (CN) near the end wall of the megagametophyte. Brightfield. X 856.

Fig. 37. Light micrograph of micropylar cytoplasm of an eight-nucleate gametophyte. Small vacuoles similar to those in chalazal cytoplasm are present. Note degenerate nucellar cells (DN) separate the micropylar end wall of the gametophyte from the inner wall of the outer integument. Brightfield. X 882.

Fig. 38. Light micrograph of ovule vasculature at eight-nucleate gametophyte stage. A sieve tube element (small arrow) has differentiated near the outer edge of the vascular strand (V). Note the terminus of the vascular strand in the dorsal segment of the outer integument (large arrows). Brightfield. X 236.

Fig. 39. Light micrograph of chalazal nucellus in an ovule with a differentiating embryo sac. Wall ingrowths (small arrows) are found on all surfaces of chalazal nucellar cells near the megagametophyte end wall. Nucellar cells at the base of the nucellus (bottom of photograph) are thin-walled and with no apparent cytological indication of degradation. Brightfield. X 957.

Fig. 40. Light micrograph of funicular vasculature at eight-nucleate gametophyte stage. Funicular vasculature (V) consists of brick-shaped cells with compact cytoplasm containing small vacuoles. No mature vascular tissue is present. Brightfield. X 380.

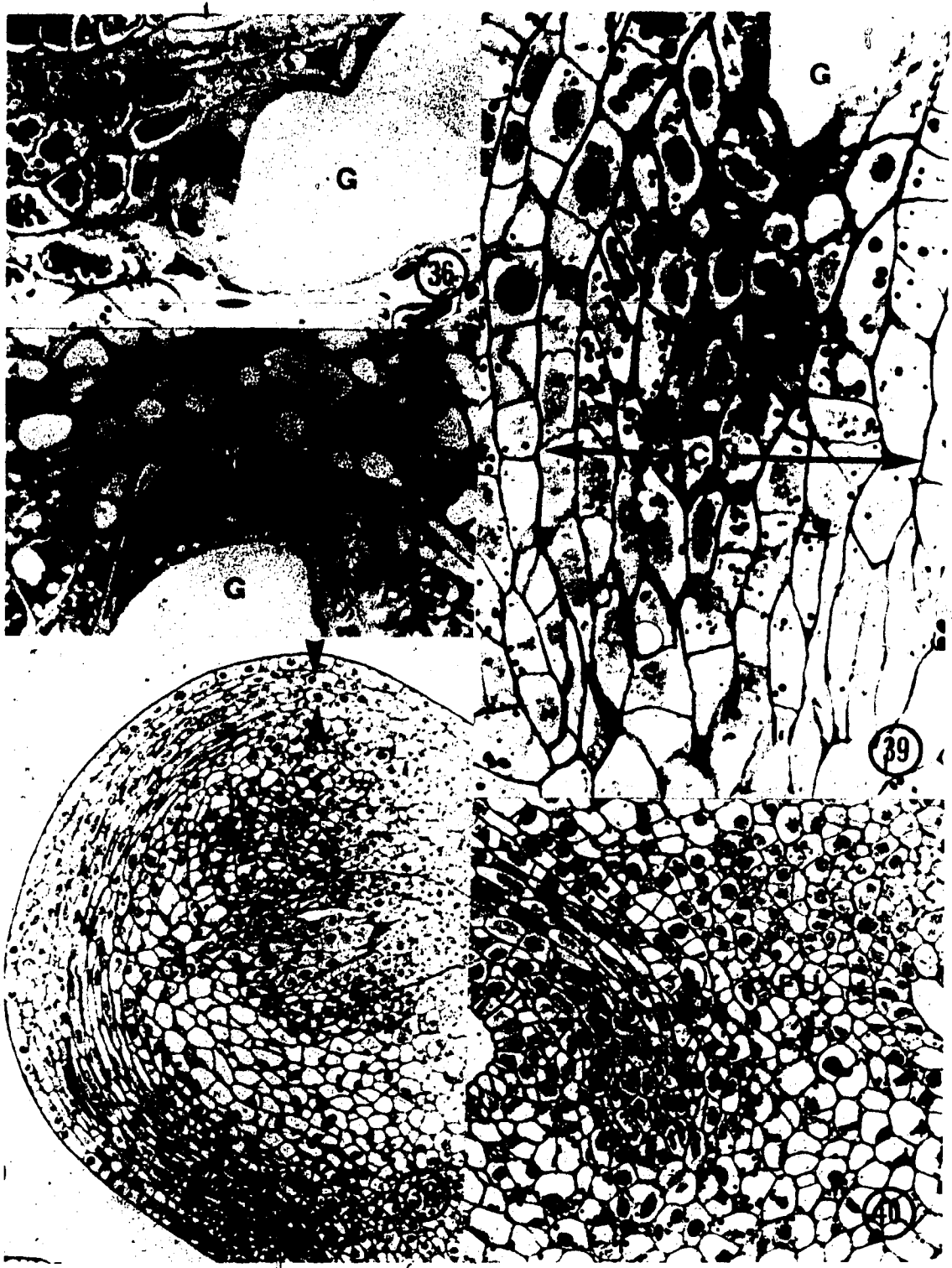


Fig. 41. Light micrograph of embryo sac. The egg apparatus (EA) is at the chalazal pole. Two polar nuclei (PN) in close proximity to each other (arrows) have migrated from the poles and occupy a mid-lateral position along the ventral wall of the megagametophyte. Three antipodal (Ant) nuclei are also apparent at the chalazal end of the megagametophyte. Paraffin embedded. Brightfield. X 380.

Fig. 42. Light micrograph of embryo sac near maturity. The distribution of embryo sac constituents (EA and PN) is similar to Fig. 41, although antipodals could not be identified and are presumed to have degenerated. Brightfield. X 148.

Fig. 43. Light micrograph of a megagametophyte after polar nucleus migration. Synergid (Syn) cells have entire walls formed. Polar nuclei (PN) are in close proximity to each other but do not fuse prior to fertilization. Note the densely ABB+ nucleoli within the polar nuclei (also see Fig. 45). Brightfield. X 624.

Fig. 44. Light micrograph of a mature embryo sac. The egg cell (E) contains a single large vacuole which laterally displaces the nucleus and cytoplasm. Most of the volume in the embryo sac is occupied by the central cell (CC) vacuole. A thin peripheral band of central cell cytoplasm borders the entire embryo sac wall. Brightfield. X 320.

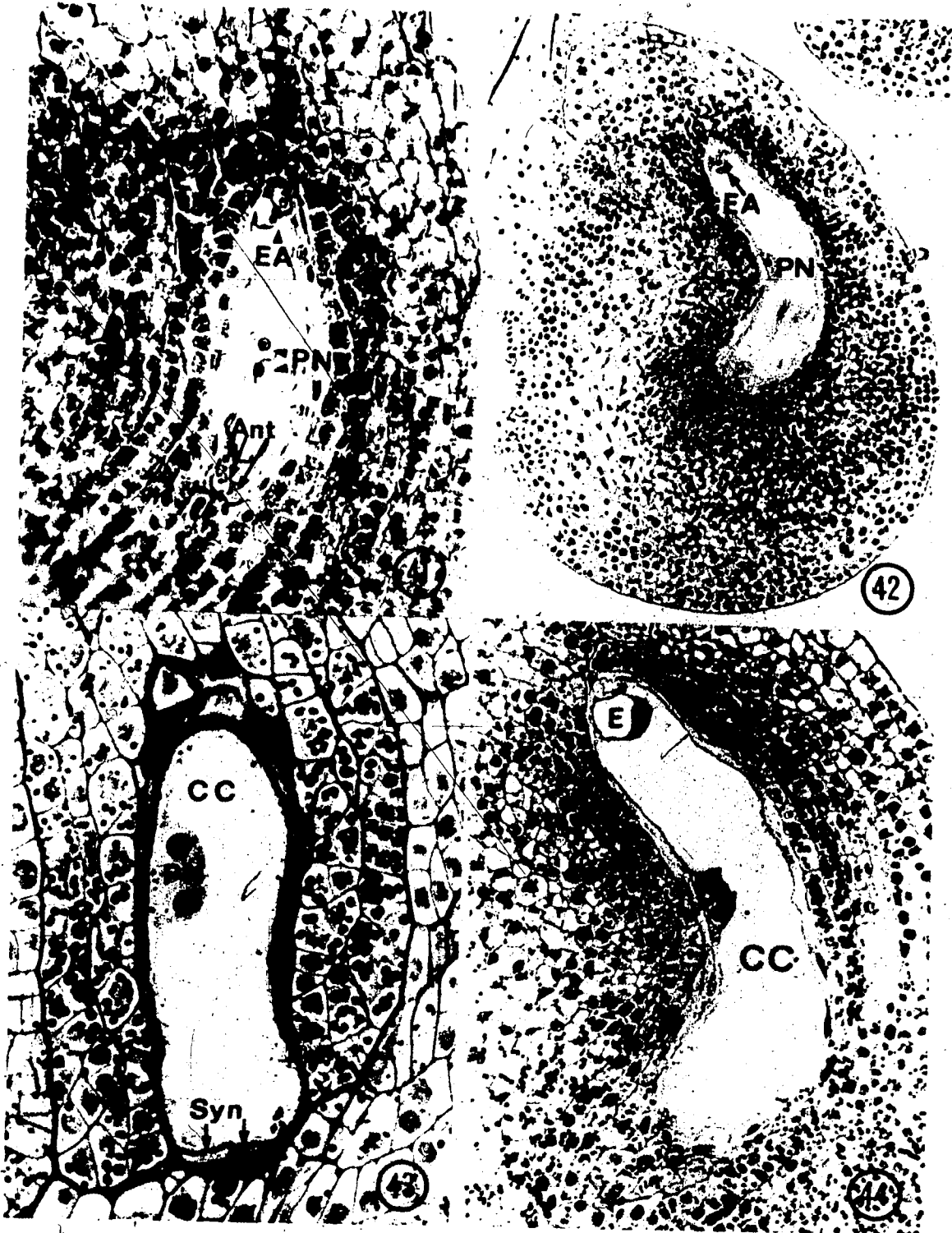


Fig. 45. Electron micrograph of polar nucleus (PN). The large electron dense vacuolate nucleolus (Nucl) occupies much of the nuclear volume. Note the degenerate nucellus (DN) separating the megagametophyte from the inner integument (II). X 8,900.

Fig. 46. Electron micrograph of rough endoplasmic reticulum (RER) in central cell cytoplasm. Strands of RER run parallel to the megagametophyte wall. X 20,150.

Fig. 47. Electron micrograph of lateral embryo sac wall (ESW). The inner surface of the wall is interrupted by embayments of central cell cytoplasm (CCC). X 26,350.

Fig. 48. Light micrograph of antipodal cells (Ant) during megagametophyte differentiation. Thin, PAS+ walls separate the antipodals from each other. Note the polar nucleus (PN) which has not yet migrated to the middle of the central cell. Brightfield. X 907.

Fig. 49. Light micrograph of chalazal end of embryo sac after antipodal degradation. The thin strip of PAS+ material is (arrows) presumed to be wall fragment. Brightfield. X 1640.

Fig. 50. Light micrograph of egg apparatus near maturity. Small vacuoles are in synergid (Syn) cytoplasm. Synergid nuclei are situated at the chalazal end of the cell. The egg (E) nucleus also occupies a chalazal position and is separated from its micropylar wall by a single large vacuole. Phase contrast. X 608.

Fig. 51. Light micrograph of micropylar cytoplasm of the megagametophyte during megagametophyte differentiation. Wall material (arrows) appears to have formed in some areas, separating the polar nucleus (PN) from cells of the egg apparatus. Brightfield. X 1560.

Fig. 52. Light micrograph of synergid cells (Syn) during megagametophyte differentiation. An entire wall separates the synergid from the central cell cytoplasm. Note the absence of wall ingrowths in the micropylar area of the wall separating the synergids (also see Fig. 54). Brightfield. X 957.

Fig. 53. Light micrographs of egg apparatus in a differentiating megagametophyte. Entire walls are formed around each of the cells. The egg cell nucleus and much of the cytoplasm are laterally displaced by a single large vacuole. Note the wall ingrowths of the synergid cells (arrow). Brightfield. X 957.

Fig. 54. Light micrograph of wall ingrowths in synergid cells of a maize egg apparatus. The inner portion is faintly PAS+, while the polysaccharide material which borders it stains darkly. Note the attachment of the egg cell (E) to the lateral wall of the embryo sac away from the immediate vicinity of the micropyle. Brightfield. X 1033.

Fig. 55. Light micrograph of wall ingrowths in the micropylar wall of a synergid cell. This thickened part of the chalazal synergid appeared to be continuous with the wall ingrowths between the synergids. Brightfield. X 756.



Fig. 56. Electron micrograph of inner integument during megagametophyte differentiation into an embryo sac. The inner and outer epidermal surfaces of the integument are covered with an electron dense material. Amyloplasts with incipient starch grains (S) are found in many of the cells. Remnants of degenerate nucellar material (DN) separate the gametophyte wall (large arrows) from the inner integument. X 3100.

Fig. 57. Light micrograph of nucellar tissue proximal to the chalazal end wall of an immature embryo sac. Nucellar cells adjacent to the embryo sac have thick, transparent walls and densely ABB+ cytoplasm. Note the nucellar cells near the nucellus-integument border do not show any characteristics of degenerate cells. Brightfield. X 705.

Fig. 58. Light micrograph of chalazal nucellus (CN) when a mature embryo sac is present. The chalazal end wall of the gametophyte is adjacent to nucellar cells with thick transparent walls. Nucellar cells (NC) extending to the nucellus-integument junction are thin-walled and contain lightly ABB+ cytoplasm with a few starch grains per cell. Brightfield. X 730.

Fig. 59. Light micrograph of transparent areas at micro-pylar ends of synergids (large arrows). The synergid wall ingrowths (small arrows) extend partly along the common walls of the two synergid cells and are probably at an early stage of formation. Brightfield. X 1440.

Fig. 60. Electron micrograph of synergid-synergid and synergid-central cell wall material. Note the irregular surface of the wall material adjacent to the plasma membranes of each cell. Plasmodesmata traverse the walls, but in some areas appear incomplete (arrows). X 13,500.



Fig. 61. Electron micrograph of degenerating nucellar cell walls. The thick wall (NCW) separating degenerating nucellar cells is electron transparent, with the exception of scattered electron dense particles in the middle lamella. X 8,990.

Fig. 62. Electron micrograph of rough endoplasmic reticulum in a degenerating nucellar cell. RER strands were usually parallel to the cell surface. X 26,950.

Fig. 63. Electron micrograph of vacuolate cytoplasm in a degenerate nucellar cell. Numerous vacuolate components of degenerating nucellar cytoplasm occur in different sizes. Dictyosomes (arrow) were rarely observed. X 16,740.

Fig. 64. Electron micrograph of inner-outer integument interface. The electron dense material (large arrows) separating the integument border consists of two separate layers each apparently derived from the integument it is associated with. Outer integument cells (OI) are elongate whereas inner integument cells (II) tend to be cuboidal. Plasmodesmata were not observed in the walls forming the border between the two integuments, but are fairly common in walls separating adjacent inner integument cells (small arrows). Note the starch grains (S) in the inner integument. X 16,740.

Fig. 65. Light micrograph of ovule vasculature in an ovule containing a mature embryo sac. A sieve tube (Ph) has differentiated at the outer edge of the vascular strand. Xylem maturation (Xy) first occurs at the inner edge of the vascular strand. Note the presence of cytoplasm in one of the xylem cells (large arrow). Brightfield. X 448.

Fig. 66. Light micrograph of funicular vasculature when a mature embryo sac is present. A sieve tube (Ph) has differentiated in the funiculus (Fu) and is continuous with the placental strand. Sieve tube elements in the funiculus are shorter than those found within the ovule (see Fig. 65). Brightfield. X 432.

Fig. 67. Electron micrograph of electron dense material (arrows) separating the inner integument (II) from degenerate nucellar cells (DN). Note how the material adjacent to the degenerate nucellus consists of alternating bands of electron dense and electron transparent material in contrast to the amorphous part contiguous with the integumentary wall. X 11,200.

Fig. 68. Light micrograph of ovule vasculature when a mature embryo sac is present. Phloem (Ph) differentiates at the outer edge, and xylem differentiates near the inner edge of the vascular cambium (see Fig. 65). Transverse section. Brightfield. X 347.



Fig. 73. Fluorescence micrographs of ovules stained with acridine orange.

Fig. 69. Ovule at the megaspore mother cell stage. The distinctive nucleolus (Nucl) of the megaspore mother cell (MMC) fluoresced faintly, and not apparently brighter than its primary fluorescence without acridine orange treatment. X 211.

Fig. 70. Ovule with an enlarging functional megaspore (FM). Within the functional megaspore, no cytoplasmic fluorescence was observed; only the nucleolus fluoresced brightly. Note the strong fluorescence of two micropylar degenerating megaspores (DM) and the lack of similar fluorescence in the adjacent megaspore (large arrow). X 236.

Fig. 71. Ovule at the four-nucleate gametophyte stage. Walls of the nucellar epidermis (Nuc) particularly at the micropylar end and chalazal nucellar cell walls (CN) near the gametophyte (G) fluoresce brightly. The wall material of degenerative nucellar cells does not fluoresce significantly, in contrast to the brightly fluorescent cytoplasm of these cells (arrows). X 300.

Fig. 72. Ovule at the eight-nucleate gametophyte stage. As in previous stages, most of the volume of the gametophyte is occupied by a large central vacuole with no fluorescence. Short arrows point to gametophyte nuclei in the peripheral cytoplasm. The brightly fluorescent material between the lateral wall of the gametophyte and the inner integument is degenerative nucellus. Note the absence of distinctive nucellar epidermal cells in the micropylar half of the nucellus compared to Fig. 71. Thick, irregular walls of chalazal nucellar cells (CN) fluoresce brightly. This zone of cells extends radially outward to the nucellar hypodermis. Nucellar epidermal cells at the same plane do not have similar fluorescent properties. X 300.

Fig. 73. Ovule with a mature embryo sac. Traces of fluorescent material of degenerate nucellar cells are found near the lateral, micropylar surfaces and chalazal end wall of the female gametophyte.



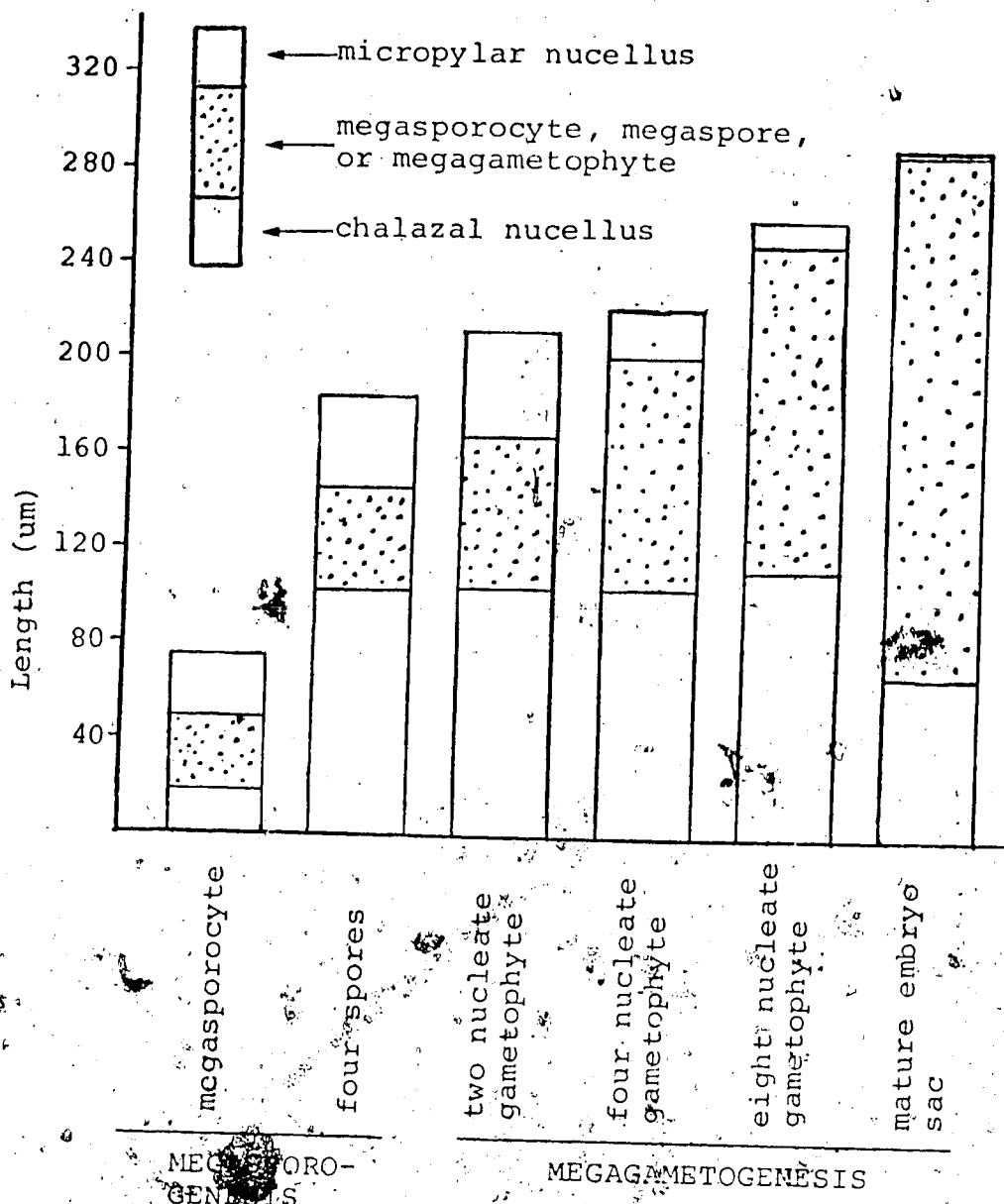


Fig. 74. Histogram of changes in nucellus, megasporocyte, functional megaspore, and megagametophyte lengths during megasporogenesis and megagametogenesis. The chalazal nucellus increases in length during megasporogenesis. Although degenerate nucellar cells are present in the chalazal nucellus, the megagametophyte does not encroach upon the chalazal nucellus until the embryo sac differentiates from an eight-nucleate coenocytic gametophyte. The increase in megagametophyte length is directed micropylarly and correlated with the degradation of micropylar nucellus. The increase in absolute length of the nucellus from chalaza to micropyle is probably due to the stretching of nucellar cells associated with megagametophyte expansion.

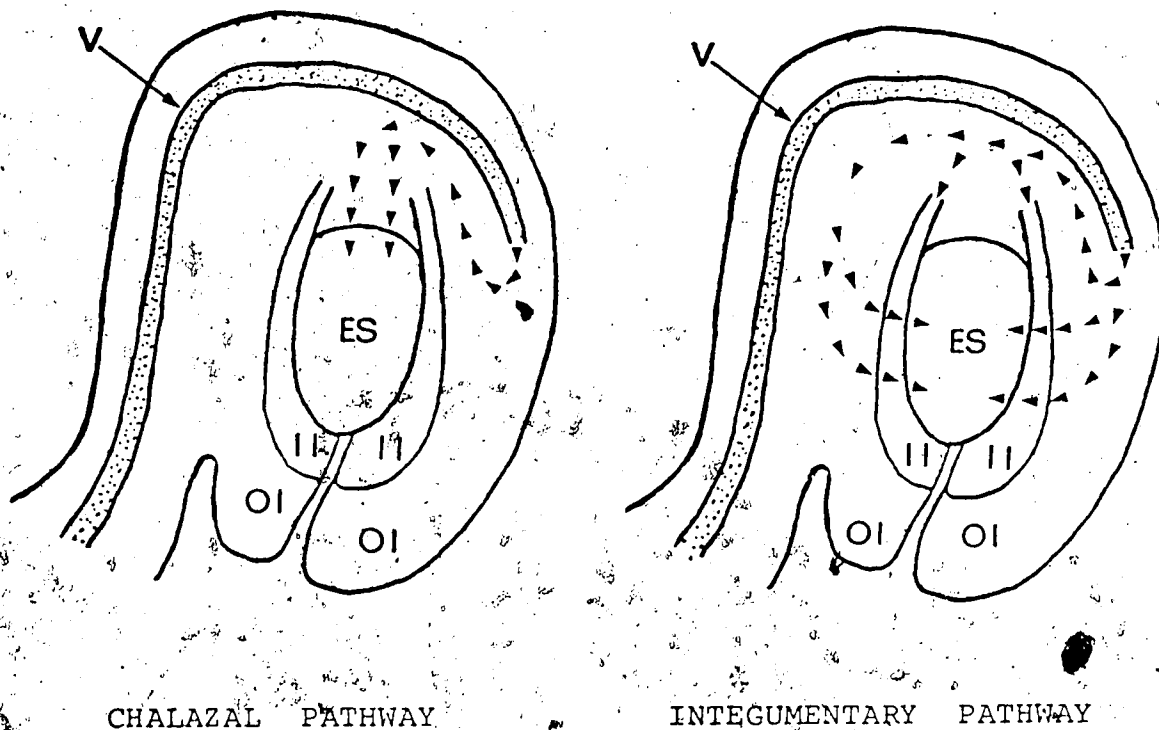


Fig. 75. Schematic representation of possible routes of nutrient transport into the embryo sac (ES). In a chalazal pathway, food materials would flow from the vascular terminus to the nucellus before reaching the embryo sac. In an endothelial (inner integument) pathway, food materials would move directly through the inner integument (II) or into the chalazal end of the integument before entering the embryo sac. (Modified after Linskens 1969).

BIBLIOGRAPHY

- Anon. 1938. Calif. Agr. Expt. Sta. Circ. 347.
- Armstrong, J.A. 1956. A histochemical differentiation of nucleic acids by means of induced fluorescence. Exp. Cell Res. 11: 640-643.
- Benson, M. 1894. Contribution to the embryology of the Amentiferae I. Trans. Linn. Soc. London, II Bot. 3: 409-424.
- _____, E. Sandy, and E. Berridge 1906. Contribution to the embryology of the Amentiferae II Carpinus betulus. Trans. Linn. Soc. London, II Bot. 7: 37-44.
- Birnstiel, M.L., M.I.H. Chipchase, and R.J. Hayes 1962. Incorporation of L-(C-14) leucine by isolated nuclei. Biochim. Biophys. Acta. 55: 728-734.
- _____, and W.G. Flamm 1964. Intranuclear site of histone synthesis. Science 145: 1435-1437.
- Brink, R.A. and D.C. Cooper 1944. The antipodals in relation to abnormal endosperm behavior in Hordeum jubatum X Secale cereale hybrid seeds. Genetica 29: 391-406.
- Cass, D.D. 1972. Occurrence and development of a filiform apparatus in the egg of Plumbago capensis. Amer. J. Bot. 59(3): 279-283.
- _____, and W.A. Johnson 1970. Fertilization in barley. Amer. J. Bot. 57: 62-70.
- Cooper, D.C. 1937. Microsporogenesis and development of the embryo sac of Lilium henryi. Bot. Gaz. 97: 346-355.
- _____. 1938. Embryology of Pisum sativum. Bot. Gaz. 100: 123-132.
- Cooper, G.O. 1938. Cytological investigations of Pisum sativum. Bot. Gaz. 99: 584-591.
- _____. 1942. Microsporogenesis and development of seed in Lobelia cardinalis. Bot. Gaz. 104: 72-81.
- Davis, G. 1966. Systematic Embryology of the Angiosperms. John Wiley and Sons, Inc., New York.
- Diboll, A.G. 1968. Fine structural development of the megagametophyte of Zea mays following fertilization. Amer. J. Bot. 55: 787-806.

- _____ and D.A. Larsen 1966. An electron microscopic study of the mature megagametophyte in Zea mays. Amer. J. Bot. 53: 391-402.
- Dupraw, E.J. 1968. Cell and Molecular Biology. Academic Press, New York.
- Esau, K. 1965. Plant Anatomy 2nd ed. John Wiley & Sons, Inc., New York.
- Fagerlind, F. 1947. Gynocummorphologische and embryologische studien in der familie Olacaceae. Bot. Notiser. 207-230.
- Fisher, D.B. 1968. Protein staining of ribboned epon sections for light microscopy. Histochemie 16: 92-96.
- Foster, A.S. and E.M. Gifford, Jr. 1959. Comparative Morphology of Vascular Plants. W.H. Freeman and Co., San Francisco.
- Frye, T.S. 1902. A morphological study of certain Asclepiadaceae. Bot. Gaz. 34: 389-413.
- Gunning, B.E.S., J.S. Pate, and L.G. Briarty 1968. Specialized "transfer cells" in minor veins of leaves and their possible significance in phloem translocation. J. Cell Biol. 37: C7-C12.
- _____ and J.S. Pate 1969. "Transfer cells" plant cells with wall ingrowths, specialized in relation to short distance transport of solutes-their occurrence, structure, and development. Protoplasma 68: 107-133.
- Jacobsen, J.V. and J.E. Varner 1967. Gibberellic acid-induced synthesis of protease by isolated aleurone layers of barley. Plant Physiol. 42: 1596-1600.
- Jensen, W.A. 1965. The ultrastructure and histochemistry of the synergids in cotton. Amer. J. Bot. 52: 238-256.
- _____ 1962. Botanical Histochemistry. W.H. Freeman and Co., San Francisco.
- _____ and D.B. Fisher 1968. Cotton embryogenesis: the entrance and discharge of the pollen tube in the embryo sac. Planta (Berl) 78: 158-183.
- Johansen, D.A. 1940. Plant Microtechnique. McGraw-Hill, New York.
- Johri, B.M. 1962. Nutrition of the embryo sac. In: Proc. Summer School Bot., Darjeeling. (Eds. P. Maheshwari, et al): 106-118.

- Joshi, A.C. and J. Venkateswarlu 1935. Embryological studies in the Lythraceae I. Lawsonia inermis Linn. Proc. Indian Acad. Sci. B2: 481-493.
- _____, _____ 1936. Embryological studies in the Lythraceae III. Proc. Indian Acad. Sci. B3: 377-400.
- Kajale, L.B. 1944. A contribution to the life history of Zizyphus jujuba Lamk. Proc. Nat. Inst. Sci. India 10: 387-391.
- Kausik, S.B. 1935. The life history of Lobelia trigona Roxb. with special reference to the nutrition of the embryo sac. Proc. Indian Acad. Sci. B2: 410-418.
- Linskens, H.F. 1969. Fertilization mechanisms in higher plants. In: Metz, C.B. and A. Monroy (eds.) Fertilization. Chapt. 5. Academic Press, New York.
- Maheshwari, P. 1948. The angiosperm embryo sac. Bot. Rev. 14:1-56.
- _____, _____ 1950. An introduction to the Embryology of Angiosperms. McGraw-Hill Book Company, Toronto.
- Marinos, N.G. 1970a. Embryogenesis of the pea (Pisum sativum) I. The cytological environment of the developing embryo. Protoplasma 70: 261-279.
- _____, _____ 1970b. Embryogenesis of the Pea (Pisum sativum) II. An unusual type of plastid in the suspensor cells. Protoplasma 71: 227-233.
- Masand, P. and R.N. Bapil 1966. Nutrition of the embryo sac and embryo—a morphological approach. Phytomorph. 16: 158-175.
- Newcomb, W.F. 1972. The development of the embryo sac of sunflower Helianthus annuus L. before and after fertilization. Ph.O. Thesis University of Saskatchewan, Saskatoon, Sask.
- _____, _____ and T.A. Steeves 1971. Helianthus annuus embryogenesis. Embryo-sac wall projections before and after fertilization. Bot. Gaz. 132: 367-371.
- Nobel, P.S. 1974. Biophysical Plant Physiology. W.H. Freeman and Co., San Francisco.
- Paleg, L. 1960. Physiological effects of gibberellic acid. II. on starch hydrolyzing enzymes of barley endosperm. Plant Physiol. 35: 902-906.

- _____ 1965. Cellular localization of the gibberellin-induced response of barley endosperm. *Colloq. Int. Centre. Nat. Res. Sci.* 123: 303-317.
- Pate, J.S., B.E.S. Gunning, and F.F. Milliken 1970. Function of transfer cells in the nodal regions of stems, particularly in relation to nutrition of young seedlings. *Protoplasma* 71: 313-334.
- _____, _____ 1969. Vascular transfer cells in angiosperm leaves—a taxonomic and morphological survey. *Protoplasma* 68: 135-156.
- _____, _____ 1972. Transfer cells. *Ann. Rev. Plant Physiol.* 23: 173-196.
- Reeve, R.M. 1948. Late embryogeny and histogenesis in *Pisum*. *Amer. J. Bot.* 35: 591-602.
- Reynolds, E.S. 1963. The use of lead citrate at high pH as an electron-opaque stain in electron microscopy. *J. Cell Biol.* 17: 208-212.
- Roy, B. 1933. Studies in the development of the female gametophyte in some leguminous crop plants of India. *Indian Jour. Agr. Sci.* 3(b): 1098-1107.
- Sass, J.E. 1958. *Botanical Microtechnique*. The Iowa State University Press, Ames, Iowa.
- Schulz, R. and W.A. Jensen 1968a. *Capsella* embryogenesis: the synergids before and after fertilization. *Amer. J. Bot.* 55: 541-552.
- _____, _____ 1968b. *Capsella* embryogenesis: the egg, zygote, and young embryo. *Amer. J. Bot.* 55: 807-819.
- _____, _____ 1969. *Capsella* embryogenesis: The suspensor and basal cell. *Protoplasma* 67: 138-163.
- Sirlin, J.L. 1960. Cell sites of RNA and protein synthesis in the salivary gland of *Smittia* (Diptera: Sironomidae). *Exp. Cell Res.* 19: 177-180.
- Spurr, A.R. 1969. A low-viscosity epoxy resin embedding medium for electron microscopy. *J. Ultrastruc. Res.* 26: 31-43.
- Steiner, A.A. and J. van Winden 1969. Recipe for ferric salts of ethylenediaminetetraacetic acid. *Plant Physiol.* 46: 862-863.
- Subramanyam, K. 1960. Nutritional mechanism of the seed. I. Nutritional mechanism of the embryo sac. *J. Madras Univ.* XXX B(1): 29-44.

- Torosian, C.D. 1971. Ultrastructure of endosperm haustorial cells of *Lobelia* Green (Campanulaceae, Lobelioideae). *J. Bot.* 5: 456-457. (Abstr.).
- Van der Pluijm, J.E. 1964. An electron microscopic investigation of the filiform apparatus in the embryo sac of *Torenia fournieri*. In: *Pollen Physiology and Fertilization*. J.F. Linskens (ed.) North-Holland Publishing Co. Amsterdam. pp. 8-16.
- Varner, J.E. 1964. Gibberellic acid controlled synthesis of α -amylase in barley endosperm. *Plant Physiol.* 39: 413-415.
- _____ and G. Ram Chandra 1964. Hormonal control of enzyme synthesis in barley endosperm. *Proc. nat. Acad. Sci. (Wash.)*. 52: 100-106.
- Von Bertalanffy, L. and J. Bickis 1956. Identification of cytoplasmic basophilia (ribonucleic acid) by fluorescence microscopy. *J. Histochem. Cytochem.* 4: 481-493.
- _____, L.L. Masin, and F. Masin 1956. Use of acridine orange fluorescence technique in exfoliative cytology. *Science* 124: 1024-1025.
- Wardlaw, I.F. and D.C. Mortimer 1970. Carbohydrate movement in pea plants in relation to axillary bud growth and vascular development. *Can. J. Bot.* 48(2): 229-237.
- Went, J.L. van 1970. The ultrastructure of the fertilized embryo sac of *Petunia*. *Acta Botanica Neer.* 19: 468-480.
- Whitehead, M.R. and C.A. Brown 1940. The seed of the spider lily, *Hymenocallis occidentalis*. *Amer. J. Bot.* 27: 199-203.

APPENDIX 1

STANDARD STRENGTH HOAGLAND'S SOLUTION (24 liters)

Compound	mls.
*KNO ₃	120
*Ca(NO ₃) ₂	120
*MgSO ₄	48
*KH ₂ PO ₄	24
**Micronutrients	24
***FeEDTA	24

* One molar stock solution

**² Micronutrient stock solution (1 liter):

Compound	Grams
H ₃ BO ₃	2.86
MnCl ₂ · 4H ₂ O	1.81
ZnSO ₄ · 7H ₂ O	0.222
Na ₂ MoO ₄ · 2H ₂ O	0.018
CuSO ₄ · 5H ₂ O	0.079

*** FeEDTA stock solution (1 liter):

Compound	Grams
FeSO ₄ · 7H ₂ O	24.9
KOH	16.1
Na ₂ EDTA	23.0

Bubble air into solution overnight and store in refrigerator.

END

02 05 75

FIN